SPECTRAL METHOD SOLUTION FOR SHALLOW WATER WAVE EQUATIONS

A Thesis Submitted
in Partial Fulfilment of the Requirement
for the Degree of
MASTER OF TECHNOLOGY

by

JIWESHWAR SINHA

to the

DEPARTMENT OF CIVIL ENGINEERING
INDIAN INSTITUTE OF TECHNOLOGY KANPUR
FEBRUARY, 1993

CERTIFICATE

It is certified that the work contained in the thesis entitled, " **SPECTRAL METHOD SOLUTION FOR SHALLOW WATER WAVE EQUATIONS** ", by Shri Jiweshwar Sinha, has been carried out under our supervision and this work has not been submitted elsewhere for a degree.

(DR. V. ESWARAN)

Assistant Professor

Mechanical Engineering Deptt.

IIT Kanpur

(DR. B.S. MURTY)

Assistant Professor

Civil Engineering Deptt.

IIT Kanpur

ABSTRACT

This investigation presents a Spectral Method for solving the one-dimensional shallow-water wave equations. The spectral method is based on the Chebyshev Collocation technique and a first-order finite difference time stepping. The method developed in this study is applied to route a Log-Pearson type III hydrograph through a wide rectangular channel. The spectral solutions are compared with the solutions obtained using the Preissmann finite difference scheme which is first-order accurate in space and second-order accurate in time. An error analysis is made through a parametric study. It is concluded from this study that the spectral method performs better than the Preissmann scheme as long as the time stepping errors are kept low. However, a second-order time-accurate finite difference scheme which may have only a first-order accuracy in space, performs better than a spectral method which uses first-order finite difference time stepping in cases of fast rising floods and friction dominated flows.

ACKNOWLEDGEMENT

I express my heartfelt thanks and gratitude to my guides Dr. B.S. Murty and Dr. V. Eswaran for their guidance, support and encouragement during my thesis work. They have always been ready to help me. I cannot forget the patient and sympathetic hearing that I got from them whenever I had any problems - personal or related to work. I am also grateful to all faculty of IIT Kanpur.

I thank my friends with whom I shared my enjoyments and worries. In particular, Bimal Modi, Ashok Keshri and V. Jagid have been a great help in preparation of this thesis.

Lastly, I convey my love and regards to my parents for their constant inspiration and encouragement.

Jiweshwar Sinha

Dedicated

to the

UNEMPLOYMENT

TABLE OF CONTENTS

LIST OF FIGURES

LIST OF TABLES

LIST OF SYMBOLS

General Symbols

h	flow depth
v	flow velocity
t	computational time
x	co-ordinate in the flow direction
n	Manning's coefficient of roughness
L	channel length
Δx	non-uniform grid separation
Δt	time increment
N	number of collocation or grid points
N_c	number of spectral coefficients or frequency modes
J	Jacobian
Δf	correction to solution
R	residual
T_k	Chebyshev polynomial of the first kind
c_k, c_m	specified constants
r	known quantities on R.H.S.
a-d	known quantities on L.H.S.

Special Symbols

a_o-g_o	non-dimensional constants
p_o	dimensional constant
S_r	non-dimensionlized source term
t_r	ratio of the time at C.G. of hydrograph to the time at peak discharge
t_p	time to peak discharge of inflow hydrograph
q_p	peak discharge

Greek Symbol

α	weighting factor in F.D.
β	weighting factor in F.D. preconditionar
θ	weighting factor in spectral method
ϕ	angle of channel-axis with horizontal
ω	minimum residual relaxation factor

Subscripted Symbol

sp	spectral
j	grid point
p	time level
t	partial derivative with respect to t
x	partial derivative with respect to x
o	initial uniform condition
e	exact solution

Supercript Symbol

n	number of iteration
u	upstream equation
d	downstream equation
c	continuity equation
m	momentum equation
-	non-dimensional form
'	first derivative

CHAPTER I

INTRODUCTION

Unsteady free-surface flow has been the subject of extensive studies for many decades because of its practical importance. Unsteady flow may be produced in a channel by intense rainfall (floods), by the failure of a control structures (dambreak wave), by the movement of control structures (Ex: sluice gates) in irrigation canal networks or by other natural or man-made disasters. The analysis of unsteady flow becomes important for determining the limits of potential damage due to floods, for proper design and operation of various hydraulic structures and for determining the morphological changes in the rivers. An unsteady flow analysis of a flood basically involves the determination of hydrograph at any cross-section in the channel if the hydrograph is given at an upstream location. Over the years, this analysis has progressed from an idealized analytical solution of simplified equations to the numerical models for complex situations. The numerical models involve the solution of partial differential equations describing the unsteady flow for prescribed boundary conditions. Depending on the idealization of the physical situation under study, one or more terms in the complete governing equations may be neglected.

The basic theory of unsteady flow in open-channels was first formulated by Barr'e de Saint Venant in 1871. He derived the governing equations for one-dimensional unsteady flow in prismatic channels. These equations, also known as shallow water wave equations, describe the conservation of mass and momentum and are based on the assumption of hydrostatic pressure distribution in

the vertical direction. The two governing equations are non-linear and are hyperbolic in nature. The earliest attempt at finding solutions to these equations was made by Massau in 1889 (Mahmood and Yevjevich, 1975) using graphical integration of the characteristic equations. Ritter (1892) used these equations to analytically determine the dam-break wave movement in a frictionless, horizontal, prismatic channel. Later, Dressler (1952) extended the Ritter solution to include the friction effect. However, the analytical solutions are available only for highly idealized cases and simple boundary conditions. The first engineering application of shallow water equations had to wait for the development of digital computers so that numerical techniques could be applied for solving them. The first attempt to numerically solve the one-dimensional St. Venant equations for practical problems was made by Stoker (1953) and Issacson, et al. (1954). They refined the finite difference approach of Thomas (1937) and applied it for routing floods in Ohio and Mississippi rivers. Since then, much effort has been expended in the development of the numerical techniques for solving the shallow water wave equations. These methods are well described in many text books (Mehmood and Yevjevich, 1975, Abbott, 1979, Cunge, et al., 1980 and Chaudhry, 1987) and only a brief review of literature is given below.

The characteristic method of solution was a natural choice for the early researchers because of the hyperbolic nature of the equations. One-dimensional explicit characteristic models were developed by Liggett and Woolhiser (1967), Streeter and Wylie (1967) and Ellis (1970) while the implicit characteristic models were developed by Amein (1966) and Wylie (1970). The

characteristic methods require either a curvilinear grid or interpolations in the x-t solution domain because of varying wave speed. Therefore, their application for flood routing is not popular in recent times. The characteristic method also requires special treatment in case shocks such as bores are present in the solution.

The shallow water wave equations are similar to the equations of gas dynamics. Therefore, the finite difference techniques developed in gas dynamics can be used for solving the flood routing problem also. This was first recognized by Stoker and Issacson, et al.. In a finite difference scheme, the governing equations are converted into algebraic equations by replacing the partial-differential terms by their finite difference analogs. These algebraic equations are then used to advance the solution from a known time-level to an unknown time-level. The finite difference scheme can be either explicit or implicit in nature. In an explicit finite difference scheme, the spatial derivatives and the coefficients are evaluated at the known time-level. Following the pioneering work of Lax (1954) and Lax and Wendroff (1960), several explicit finite difference models were developed for shallow water wave equations. Notable among them are those of Liggett and Woolhiser (1967), Martin and DeFazio (1969), Dronkers (1969), Strelkoff (1970) and Jhonson (1974). Many of these schemes use either the first-order time accurate Lax diffusive scheme or the second-order time accurate Leap-frog scheme (Liggett and Cunge, 1975). Recently, Fennema and Chaudhry (1986) introduced MacCormack (1969) and Gabutti (1983) schemes for the analysis of unsteady free-surface flows with shocks. Both MacCormack and Gabutti schemes are second-order accurate in time and space. All

the above explicit models have a restriction on the size of the computational time step because of numerical stability. Therefore, they are not suitable for application to routing flood waves, having a duration in order of days. This necessitated the development of implicit models.

In an implicit scheme, the solution is advanced from one time-line to the next simultaneously for all points along the time-line due to the fact that the spatial derivatives and the coefficients are evaluated at the unknown time-level. The implicit schemes are generally unconditionally stable and therefore, larger computational time steps can be used. The use of implicit models was first suggested by Issacson, et al. (1956) and became popular after the development of Preissmann four-point implicit scheme (1961). Later, Vasiliev, et al. (1965) and Abbott and Ionescu (1967) developed six-point implicit schemes. However, these schemes could not become popular because of the requirement of uniform finite difference grid. Also, the inclusion of boundary conditions is more complicated in the six-point schemes. Amein and Fang (1970) are the first to use the Newton-Raphson technique to solve the system of non-linear equations in an implicit model. Recently, Fennema and Chaudhry (1990) used the Beam and Warming implicit scheme (1976) for solving the unsteady free-surface flow problems. Notable among the other implicit models are those developed by Baltzer and Lai (1968), Fread (1973,1976) and Chen and Simons (1975).

The numerical stability and accuracy of various implicit schemes have been studied by Cunge (1966), Abbott and Ionescu (1967), Fread (1974) and Liggett, et al. (1975). Although, implicit schemes are usually unconditionally stable, Abbott and

Ionescu (1967) have demonstrated the danger of introduction of significant numerical errors when excessively large time steps are taken. A means of circumventing these errors is also described by them. Chaudhry and Contractor (1973) and Fread (1974) have shown that large computational time steps can also result in numerical instability. This is especially so when the spatial derivative terms are not sufficiently weighted towards the future time-line and the changes are rapid. Fread (1974) investigated the convergence properties of various four-point implicit schemes by determining the truncation error. The backward implicit scheme has a first-order truncation error where as the box implicit scheme has a second-order truncation error.

Taylor, et al. (1974) were probably the first to attempt at solving the shallow water equations using finite element technique. Later, Cooley and Moin (1976), King (1976), Keuning (1976) and Meissner (1978) used the finite element method based on Galerkin approach. It was concluded from their studies that the results obtained by the finite difference methods are, in general, superior to those obtained using the finite element models. Katopodes (1978,1980,1984a,b) addressed the basic difficulties encountered in the application of finite element methods for solving the shallow-water wave equations and proposed a new dissipative Galerkin scheme for open-channel flow. However, the finite element models are yet to become as popular as finite difference models at least for one-dimensional computations. They, however, are preferred by The U.S. Army Corps of Engineers (1987) in two-dimensional modeling with complex boundaries.

Both finite difference and finite element methods have only a finite-order accuracy. A considerable increase in both

algorithmic and programming complexity is involved if the order of accuracy of these methods is increased. This, however is not the case with the Spectral Method. Elaison, et al. (1970) and Gottlieb and Orszag (1977) laid the foundation of the spectral method and developed the transform method and the spectral collocation techniques. The book on spectral methods by Canuto, et al. (1987) traces the history of the methods and discusses in detail the various spectral techniques starting from first principles. The book also presents several application of spectral methods to fluid flow problems. Only a very brief review relevant to the present work is given below.

Orszag (1980) outlines the spectral collocation technique using Chebyshev polynomials and applied it to non-linear, non-constant coefficient problems. Spectral accuracy is achieved only in space while the time differencing is done by using the standard implicit finite difference schemes. Orszag (1980) also introduced the concept of preconditioning for efficiently solving the full matrix equations resulting from spectral approximation. It was shown that the extra work required in solving the spectral equations above that of solving the lowest order finite difference approximation is only O(N log N) where N is the number of grid points in the numerical scheme. Moin and Kim (1980) used a pseudo-spectral formulation based on Fourier series and Chebyshev polynomial expansions and solved some channel flow problems. A mention was made about the aliasing error but it was suggested that this error is limited due to the damping of the physical system.

In the studies reported herein, an attempt is made to develop a Spectral Method for the solution of one-dimensional

shallow-water wave equations. This spectral method is based on Chebyshev Collocation technique and finite difference time stepping. The spectral solutions for a hypothetical flood routing problem are compared with the finite difference solutions obtained using the Preissmann scheme. The spatial resolution and the time stepping errors in numerical solutions are analysed through a parametric study. In this report, the governing shallow-water wave equations and the Preissmann scheme are presented in Chapter II. In Chapters III and IV, details of Spectral Method using Chebyshev Collocation technique are presented. In Chapter V, the numerical results are discussed and an error analysis is made.

CHAPTER II

GOVERNING EQUATIONS AND THE FINITE DIFFERENCE

2.1 St. Venant Equations

The gradually varied unsteady flow in an open channel is described by the Saint Venant equations. Considering the unsteady flow in a wide rectangular prismatic channel as shown in fig 2.1, these equations are derived using the following assumptions:

(a) the flow is one-dimensional in the direction of the channel; that is, the velocity is uniform over a cross-section and the water level across a section is horizontal,

(b) vertical accelerations are negligible,

(c) steady state resistance laws may be used to model unsteady effects,

(d) the average bed slope, S_o of the channel is small such that the cosine of the angle made by the averaged bed profile with the horizontal can be regarded as unity.

By making the above assumptions, the Saint Venant equations are obtained by applying the principles of conservation of mass and conservation of momentum to a differential control volume (Chaudhry, 1986). The resulting equations in a non-conservation form are:

$$\frac{\partial h}{\partial t} + v \frac{\partial h}{\partial x} + h \frac{\partial v}{\partial x} = 0 \qquad (2.1.1a)$$

and

$$\frac{\partial v}{\partial t} + v \frac{\partial v}{\partial x} + g \frac{\partial h}{\partial x} = g (S_o - S_f) \qquad (2.1.1b)$$

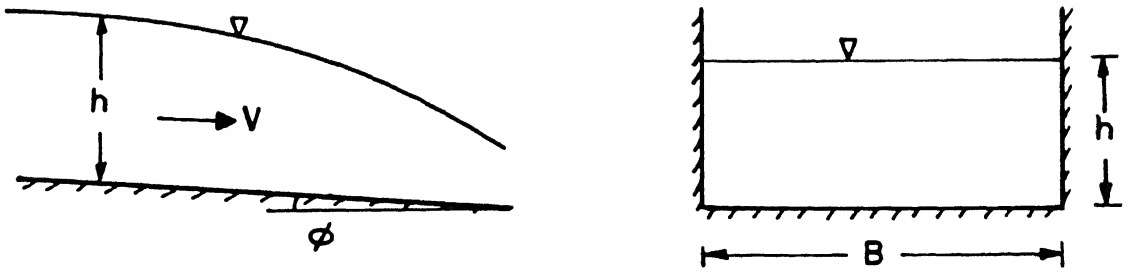

(a) Elevation (b) Cross-Section

Fig. 2·1 Definition Sketch

where h is the depth of flow; v is the flow velocity; g is the acceleration due to gravity; S_o is the slope of the channel-bottom; S_f is the slope of the energy grade line; x is the distance measured positive in the downstream direction, and t is the time of computation. In the present work, S_f is evaluated using Manning's formula for a wide rectangular channel,

$$S_f = \frac{n^2 v^2}{h^{4/3}} \qquad (2.1.2)$$

where n is the Manning's roughness coefficient.

2.2 Non-Dimensionalization

The Saint Venant equations are non-dimensionalized in the present study using channel length, L_o as distance scale parameter and the initial steady uniform flow depth, H_o as the depth scale parameter. The initial steady state uniform flow velocity, V_o is taken as the velocity scale parameter. V_o is obtained using the Manning's equation,

$$V_o = \frac{1}{n} H_o^{2/3} S_o^{1/2} \qquad (2.2.1a)$$

The time scale parameter, T_o is equal to the time required to travel a distance of L_o with a wave speed of $\sqrt{gH_o}$

$$T_o = \frac{L_o}{\sqrt{gH_o}} \qquad (2.2.1b)$$

Various dimensionless variables (barred) are defined as:

$$\bar{x} = x / L_o \qquad (2.2.2a)$$

$$\bar{t} = t / T_o \qquad (2.2.2b)$$

$$\bar{h} = h / H_o \qquad (2.2.2c)$$

$$\bar{v} = v / V_o \qquad (2.2.2d)$$

Substitution of equations (2.2.1) and (2.2.2) in equations (2.1.1) and (2.1.2) result in the following general non-dimensional St. Venant equations

$$a_o \frac{\partial \bar{h}}{\partial \bar{t}} + b_o \bar{v} \frac{\partial \bar{h}}{\partial \bar{x}} + c_o \bar{h} \frac{\partial \bar{v}}{\partial \bar{x}} = 0 \qquad (2.2.3a)$$

and

$$d_o \frac{\partial \bar{v}}{\partial \bar{t}} + e_o \bar{v} \frac{\partial \bar{v}}{\partial \bar{x}} + f_o \frac{\partial \bar{h}}{\partial \bar{x}} = g_o (S_o - p_o \bar{S}_f) \qquad (2.2.3b)$$

where a_o, b_o, c_o, d_o, e_o, f_o and g_o are dimensionless constants, but p_o is dimensional constant and it becomes dimensionless when combined with $\bar{S}_f$ where

$$\bar{S}_f = \frac{n^2 \bar{v}^2}{\bar{h}^{4/3}} \qquad (2.2.4)$$

Depending on the way the non-dimensionalization is carried out, as many as 12 variations of equation (2.2.3) are possible. The best set of equations among these is considered in the present study. The basis of selection of this set is discussed in Chapter V. Only the definitions of coefficients a_o - g_o and p_o corresponding to the best form of non-dimensional St. Venant equations are given below.

$$a_o = 1.0 \qquad (2.2.5a)$$

$$b_o = V_o T_o / L_o \qquad (2.2.5b)$$

$$c_o = b_o \qquad (2.2.5c)$$

$$d_o = V_o / gT_o \qquad (2.2.5d)$$

$$e_o = V_o^2 / gL_o \qquad (2.2.5e)$$

$$f_o = H_o / L_o \qquad (2.2.5f)$$

$$g_o = 1.0 \qquad (2.2.5g)$$

and

$$p_o = V_o^2 / H_o^{4/3} \qquad (2.2.5h)$$

The right hand term of the equation (2.2.3b) is a source term which is highly non-linear in nature and requires a different treatment. Therefore, it is represented by a special symbol $\bar{S}_r$.

$$\bar{S}_r = g_o(S_o - p_o \bar{S}_f) \qquad (2.2.6)$$

2.3 Preissmann Scheme

The governing equations presented in the previous section constitute a set of non-linear, first-order, hyperbolic partial differential equations, analytical solutions for which are

available only for highly idealized cases. Therefore, they are generally solved using numerical techniques. In this section, one such scheme, originally developed by Preissmann (1961), is presented.

Preissmann scheme (1961) is basically a four-point weighted implicit finite difference scheme. It is used to transform the non-linear partial differential equations of St. Venant into non-linear algebraic equations. Referring to fig. 2.2, a function f(x,t) is represented by its values on a grid with F_j^p denoting the value at the jth grid point and the pth time level. Δx_j is the non-dimensional grid spacing between the (j+1)th and the jth point. Then for a non-dimensional time step Δt, the four-point weighted difference approximations for the time and space derivatives f_t and f_x for a "cell" defined by the four points (p,j), (p+1,j), (p,j+1), (p+1,j+1) are

$$f_t = \frac{f_{j+1}^{p+1} - f_{j+1}^{p} + f_j^{p+1} - f_j^{p}}{2\Delta t} \qquad (2.3.1a)$$

$$f_x = \alpha \left[\frac{f_{j+1}^{p+1} - f_j^{p+1}}{\Delta x_j}\right] + (1-\alpha) \left[\frac{f_{j+1}^{p} - f_j^{p}}{\Delta x_j}\right] \qquad (2.3.1b)$$

and

$$f(x,t) = \alpha \left[\frac{f_{j+1}^{p+1} + f_j^{p+1}}{2}\right] + (1-\alpha) \left[\frac{f_{j+1}^{p} + f_j^{p}}{2}\right] \qquad (2.3.1c)$$

where α is a weighting factor varying from 0.5 to 1.

A scheme using an α value of 0.5 is known as the 'box scheme' while $\alpha = 1$ results in the 'fully implicit scheme'. For $\alpha = 0.5$, the scheme is of second-order accurate in time, otherwise

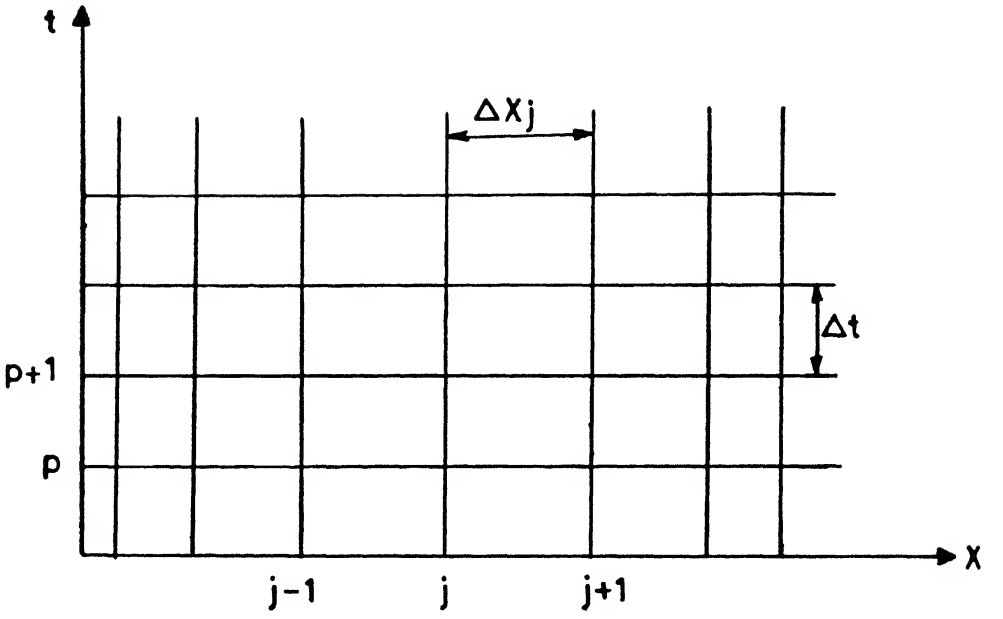

Fig. 2·2 Computational Grid

it remains first-order accurate. Fread (1974) recommends α values nearer to 0.5 to insure unconditional linear numerical stability and also provide good accuracy.

2.3.1 Boundary Conditions

The four-point implicit scheme presented in the previous section is based on forward finite differencing. Therefore, from N nodes only (2N-2) algebraic equations are obtained using the St. Venant equations (2.2.3). However, the number of unknowns at the advanced time level are 2N. The additional two equations required for completely solving the system are obtained from boundary conditions. The specification of boundary conditions depends on whether the flow is subcritical or supercritical. In the present work, we are interesed only in the case of subcritical flows. Therefore, one boundary condition is specified at the upstream end and another is specified at the downstraem end (Stoker 1957).The upstream boundary condition is specified by a hydrograph (typically of type III) and a second order extrapolation $\partial^2 h / \partial x^2 = 0$ is applied at the downstream end.

The general form of the type III hydrograph is represented by

$$q(t) = q_o\left[1+(q_p-1)(t/t_p)^{[1/(t_r-1)]}\, e^{[1-(t/t_p)][1-(t_r-1)]}\right] \qquad (2.3.1.1)$$

in which q(t) is the discharge per unit width at time t; q_o is the initial discharge; t_p is the time at which peak discharge occurs; q_r is the ratio of discharge at peak to initial discharge and t_r is the ratio of time at Centre of Gravity of the hydrograph to the

time of peak discharge.

The second order extrapolation ($\partial^2 h / \partial x^2 = 0$) at the downstream end results in the following equation,

$$(x_N - x_{N-1})h_{N-2} - (x_N - x_{N-2})h_{N-1} + (x_{N-1} - x_{N-2})h_N = 0 \qquad (2.3.1.2)$$

where subcript represents the grid-point.

It should be noted here that the above second-order extrapolation at the downstream end is strictly not valid. However, it gives proper results as long as we are not interested in the upstream effects of the downstream boundary. Therefore, the above methodology can be used only for routing floods in channel reaches which are away from dams, weirs, channel junctions etc. In such cases, a rating curve at the downstream end can be used as a boundary condition.

2.3.2 Algorithm

Equations (2.2.3) are discretized using the equations (2.3.1). This results in a system (2N-2) of non-linear algebraic equations corresponding to N grid points. Two separate non-linear algebraic equations are obtained from upstream and downstream boundary conditions (2.3.1.1) and (2.3.1.2). The system of equations can be represented in a functional form as given below,

$$B_1 (\bar{h}_1, \bar{v}_1) = 0 \qquad (2.3.2.1a)$$

$$C_j (\bar{h}_j, \bar{v}_j, \bar{h}_{j+1}, \bar{v}_{j+1}) = 0 , \qquad 1 \le j \le N-1 \qquad (2.3.2.1b)$$

$$M_j (\bar{h}_j, \bar{v}_j, \bar{h}_{j+1}, \bar{v}_{j+1}) = 0 , \qquad 1 \le j \le N-1 \qquad (2.3.2.1c)$$

and

$$B_N\ (\bar{h}_{N-2},\ \bar{h}_{N-1},\ \bar{h}_N) = 0 \qquad (2.3.2.1d)$$

where subscript denotes the grid-point and the barred notation is for the normalized value of the variable. In (2.3.2.1) C and M correspond to the functional form of the discretized St. Venant equations and B corresponds to the functional form of boundary conditions. Complete details of these equations are presented in the Appendix A.

The non-linear equations (2.3.2.1) are solved in this study using Newton-Raphson method. The Newton-Raphson method is basically a functional iterative technique to solve a system of non-linear equations. This technique is derived from a Taylor series expansion of the non-linear function in which all terms of second and higher order are neglected. The resulting algorithm is,

$$J\ (f^n)\ \Delta f = -\ F(f^n) \qquad (2.3.2.2)$$

in which f^n is a vector quantity, J is the Jacobian (a coefficient matrix made up of the partial derivatives evaluated with f^n values), $F(f^n)$ is the non-linear vector equation evaluated with f^n values, and Δf is a vector containing the 2N unknowns. Equation (2.3.2.2) represents a system of equations in which the unknown vector Δf is linear . Thus, the Newton-Raphson method generates a 2N x 2N matrix equation. This matrix is banded with most of the elements being zero except for four elements in each row along the main diagonal of the matrix. In the present work, application of

the Newton-Raphson method to the equation (2.3.2.1) results in the following matrix equation.

$$\begin{bmatrix} a_1^u & b_1^u & 0 & 0 & 0 & 0 & 0 & 0 & 0 & 0 \\ a_1^c & b_1^c & c_2^c & d_2^c & 0 & 0 & 0 & 0 & 0 & 0 \\ a_2^m & b_2^m & c_2^m & d_2^m & 0 & 0 & 0 & 0 & 0 & 0 \\ 0 & 0 & a_2^c & b_2^c & c_3^c & d_3^c & 0 & 0 & 0 & 0 \\ 0 & 0 & a_2^m & b_2^m & c_3^m & d_3^m & 0 & 0 & 0 & 0 \\ 0 & 0 & 0 & 0 & \cdots & \cdots & \cdots & \cdots & 0 & 0 \\ 0 & 0 & 0 & 0 & \cdots & \cdots & \cdots & \cdots & 0 & 0 \\ 0 & 0 & 0 & 0 & 0 & 0 & a_{N-1}^c & b_{N-1}^c & c_N^c & d_N^c \\ 0 & 0 & 0 & 0 & 0 & 0 & a_{N-1}^m & b_{N-1}^m & c_N^m & d_N^m \\ 0 & 0 & 0 & 0 & a_{N-2}^d & 0 & a_{N-1}^d & 0 & a_N^d & 0 \end{bmatrix} \begin{bmatrix} \Delta h_1 \\ \Delta v_1 \\ \Delta h_2 \\ \Delta v_2 \\ \Delta v_3 \\ \cdots \\ \cdots \\ \\ \Delta h_N \\ \Delta v_N \end{bmatrix} = \begin{bmatrix} r_1^u \\ r_1^c \\ r_1^m \\ r_2^c \\ r_2^m \\ \cdots \\ \cdots \\ r_{N-1}^c \\ r_{N-1}^m \\ r_N^d \end{bmatrix} \qquad (2.3.2.3)$$

In the above equation, coefficients a_j^c, b_j^c, c_j^c and d_j^c are partial differentials of the discretized continuity equation (2.3.2.1b) with respect to h_j^{p+1}, v_j^{p+1}, h_{j+1}^{p+1} and v_{j+1}^{p+1} respectively; coefficients a_j^m, b_j^m, c_j^m and d_j^m are partial differentials of normalized dynamic equation (2.3.2.1c) with respect to h_j^{p+1}, v_j^{p+1}, h_{j+1}^{p+1} and v_{j+1}^{p+1} respectively; coefficients a_1^u and b_1^u are partial differentials of the normalized upstream boundary condition (2.3.2.1a) with respect to h_1^{p+1} and v_1^{p+1} respectively; coefficients a_{N-2}^d, a_{N-1}^d and a_N^d are partial differentials of the normalized downstream boundary condition (2.3.2.1d) with respect to h_{N-2}^{p+1}, h_{N-1}^{p+1} and h_N^{p+1} respectively. r_1^u, r_j^c, r_j^m and r_N^d are the residuals obtained from upstream boundary condition (2.3.2.1a), continuity equation (2.3.2.1b), momentum equation (2.3.2.1c) and downtream boundary condition (2.3.2.1d) at time level (p+1) respectively. Complete details of the coefficients are presented in the Appendix B.

The solution of St. Venant equations by a finite difference scheme essentially involves determining the depth and velocity values at all the grid points at the unknown, (p+1) time level using the depth and velocity values at the grid points at the known, (p) time level. This is accomplished using the following procedure.

(a) Assume values of h_j^{p+1}, v_j^{p+1} for all j = 1 to N.

(b) Use h_j^p, v_j^p, h_j^{p+1} and v_j^{p+1} to determine r_1^u, r_j^c, r_j^m, r_N^d and the elements of the coefficient matrix in the equation (2.3.2.3).

(c) Determine Δh_j and Δv_j for all j = 1 to N by solving the matrix equation (2.3.2.3). A standard library subroutine is used for this purpose.

(d) The corrections Δh_j and Δv_j are added to h_j^{p+1} and v_j^{p+1} to get the new guess values for h_j^{p+1} and v_j^{p+1}. This entire process is repeated till convergence.

(e) The values of h_j^{p+1} and v_j^{p+1} obtained after the convergence are referred to as the finite difference solutions of the St. Venant equations.

(f) Once the solution is obtained at the (p+1) time level, it is advanced to the next time level and the procedure is repeated till the end of simulation period is reached.

The finite difference solution at any time forms the initial guess for the Spectral solution at that time. The basics of Spectral method are presented in Chapter III and the complete algorithm is discussed in Chapter IV.

CHAPTER III

SPECTRAL METHOD

This chapter contains the details of the spectral method including Chebyshev polynomials, the Chebyshev-Collocation techniques and the Preconditioned Residual Minimization method.

3.1 The Collocation Method

The spectral collocation technique is generally used for solving fluid flow problems. The technique uses expansion functions such as orthogonal Chebyshev and Legendre' polynomials, and treats the function values at certain physical points as the fundamental representation of the solution.

In the Collocation approach, the truncated series of the solution is represented as;

$$h_N(x) = \sum_{k=0}^{N_c-1} \hat{h}_k B_k(x) , \qquad -1 \le x \le 1 \qquad (3.1.1)$$

where h_N is the spectral representation of h, $\hat{h}_k$ are the spectral coefficients, B_k are the orthogonal expansion functions and N_c is the number of terms in the expansion.

For any differential equation

$$M(h) = f(x) , \qquad -1 \le x \le 1 \qquad (3.1.2)$$

where M(h) is a differential operator which includes spatial derivatives of h, and f is the known forcing function. If the approximate solution (3.1.1) does not satisfy (3.1.2) everywhere, then the residual

$$R_N(x) = f_N(x) - M_{sp}(h_N) \qquad (3.1.3)$$

does not vanish everywhere. In (3.1.3) f_N and M_{sp} are the spectral approximations of f(x) and M(h) respectively. For the collocation method, the prime requirement is that the P.D.E. be satisfied exactly at each of the collocation points x_j, i.e.

$$f_N(x) - M_N(h_N)\Big|_{x=x_j} = 0 , \qquad j = 1,2,\ldots,N \qquad (3.1.4)$$

The spectral coefficients $\hat{h}_k$ can be found either by analytic integration using the orthogonal property of the basis functions or by finite transformation which relate the coefficients to the function values at collocation points. The first approach is called the " Galerkin " and the second the " Collocation ".

3.2 Chebyshev Polynomials and Evaluation of Derivatives

The Chebyshev polynomials are a family of orthogonal polynomials in the interval (-1,1). Chebyshev polynomials satisfy the orthogonal relationship,

$$\int_{-1}^{1} \frac{T_k(x)\, T_m(x)}{\sqrt{1 - x^2}}\, dx = \frac{\pi}{2} C_k\, \delta_{km} , \text{ where } C_k = \begin{cases} 2 \text{ if } k = 0 \\ 1 \text{ otherwise} \end{cases} \qquad (3.2.1)$$

where $T_k(x)$ are the Chebyshev polynomials of the first kind. If the approximate solution $h_N(x)$ is represented as

$$h_N(x) = \sum_{k=0}^{N_C - 1} \hat{h}_k\, T_k(x) \qquad (3.2.2)$$

then using (3.2.1) the equation for the Chebyshev coefficients becomes

$$\hat{h}_m = \frac{1}{\bar{C}_m} \int_{-1}^{1} \frac{h_N(x)\, T_m(x)}{\sqrt{1 - x^2}}\, dx \qquad (3.2.3)$$

The Gauss-Lobatto quadrature rule which provides a means of representing the continuous integral of a function in terms of a discrete summation, gives the Chebyshev-Gauss-Lobatto Collocation points

$$x_j = \cos\left[\frac{\pi\, j}{N}\right] \qquad (3.2.4)$$

Thus the spectral coefficients are determined by the forward transformation;

$$\hat{h}_k = \sum_{j=1}^{N} C_{kj}\, h_j \qquad k = 0,1,2,\ldots,N_c-1 \qquad (3.2.5)$$

where h_j are the values of the function at the collocation points x_j and

$$C_{kj} = \frac{2}{(N-1)\,\bar{C}_j\,\bar{C}_k} \cos\left[\frac{\pi(j-1)k}{N-1}\right] \qquad \begin{matrix} j = 1,2,\ldots,N \\ k = 0,1,2,\ldots,N_c-1 \end{matrix} \qquad (3.2.6)$$

where

$$\bar{C}_j = \begin{cases} 2 & j = 1,N \\ 1 & 2 \le k \le N-1 \end{cases} \quad \& \quad \bar{C}_k = \begin{cases} 2 & k = 1,N_c-1 \\ 1 & 2 \le k \le N_c-2 \end{cases} \qquad (3.2.7)$$

The grid point values of the function can be obtained from the spectral coefficients by the inverse transformation given by

$$h_j = \sum_{k=0}^{N_c-1} C^{-1}_{kj} \hat{h}_k \qquad j = 1,2,\ldots,N \qquad (3.2.8)$$

where the inverse transformation matrix is defined as

$$C^{-1}_{kj} = \cos\left\{\frac{\pi(j-1)k}{N-1}\right\} \qquad \begin{matrix} j = 1,2,\ldots,N \\ k = 0,1,2,\ldots,N_c-1 \end{matrix} \qquad (3.2.9)$$

Both the forward and the inverse transforms can be implemented by using either Matrix Multiplication or the Fast Fourier Transform depending upon the number of coefficients and the number of grid points.

The derivatives of the function h having Chebyshev polynomials can be written as

$$h'_N = \sum_{k=0}^{\infty} \hat{h}^{(1)}_k T_k(x) \qquad (3.2.10)$$

where $\hat{h}^{(1)}_k$ are the spectral coefficients of the derivative. From the relationship,

$$2\, T_k(x) = \frac{1}{k+1} T'_{k+1}(x) - \frac{1}{k-1} T'_{k-1}(x), \qquad k \geq 1 \qquad (3.2.11)$$

we can obtain the recurrence relationship

$$2k\, \hat{h}_k = C_{k-1}\, \hat{h}^{(1)}_{k-1} - \hat{h}^{(1)}_{k+1}, \qquad k \geq 1 \qquad (3.2.12)$$

This relation gives an efficient way of differentiating a polynomial of degree N in Chebyshev space. Since $\hat{h}^{(1)}_k = 0$ for $k \geq N_c-1$, the non-zero coefficient are computed in decreasing order by the recurrence relation;

$$C_k \hat{h}_k^{(1)} = \hat{h}_{k+2}^{(1)} + 2(k+1)\hat{h}_{k+1}, \quad 0 \le k \le N_c-1 \qquad (3.2.13)$$

After knowing the coefficients of h, the coefficients of the derivative of the function can be known using (3.2.13). These coefficients are then transformed back into physical space using an Inverse Transform to obtain the grid point values of the derivative. By this way a very accurate approximation of the derivatives of the function is determined.

3.3 The Chebyshev-Collocation Method with F.D. Time Stepping

Let us apply the Chebyshev-Collocation method to the equation

$$h_t = M(h), \qquad -1 \le x \le 1 \qquad (3.3.1)$$

where M(h) is the differential operator containing spatial derivatives of h(x,t) and h_t is the partial derivatives of h with respect to time.

The Chebyshev expansion of a function h(x,t) in the interval (-1,1) is given by

$$h(x,t) = \sum_{k=0}^{\infty} \hat{h}_k(t)\, T_k(x) \qquad (3.3.2)$$

If the function h(x,t) is infinitely differentiable on (-1,1), then the Chebyshev coefficients decay faster than algebraically for increasing k. This ensures the spectral accuracy of the method.

In practice, the truncated series of the solution is

represented as

$$h_N(x,t) = \sum_{k=0}^{N_c-1} \hat{h}_k(t)\, T_k(x) \quad , \quad -1 \le x \le 1 \qquad (3.3.3)$$

where N_c is the number of modes.

In solving (3.3.1) by a spectral method, the time derivative is discretized by finite difference technique. For a simple implicit time-stepping scheme, (3.3.1) can be approximated as

$$h_j^{p+1} = h_j^p + \Delta t \left[M_{sp}\,(h_N^{p+1}) \right]_j \quad , \quad j = 1,2,\ldots,N \qquad (3.3.4)$$

where the subscript j refers to the values at the collocation points x_j and the superscript p refers to the time-level. The number of points N is equal to the number of coefficients N_c. The operation $M_{sp}(h_N)$ is evaluated spectrally at the collocation points by using the collocation method explained in the previous section.

The scheme (3.3.4) requires an iterative process for obtaining the solution because of the unknown h_j^{p+1} presents in the spectral operator M_{sp}. However the spectral operator M_{sp} is generally difficult and expansive to invert. This difficulty is circumvented by adopting finite difference approximation of the spectral operator for use in the iterative solution of (3.3.4). The approximate operator is chosen such that it is close to the original spectral operator and is inexpensive and easy to invert. This is known as Preconditioning. This preconditioning reduces the computational cost of the iterative solution procedure.

3.4 Preconditioned Residual Minimization

Preconditioned residual minimization is the basis of the iterative algorithm used in the present work. This technique is briefly explained here. Let us consider a spectral equation as :

$$M_{sp}(h) = f \qquad (3.4.1)$$

where M_{sp} is the spectral representation of a differential operator M and f is a known forcing function.

For any guess solution h^n, the residual in the equation is determined as

$$R^n = f - M_{sp}(h^n) \qquad (3.4.2)$$

The next step is to evaluate the corrections Δh^n to be applied to the solution. This is done by using a finite difference solver. To ensure rapid minimization of the residual and to accelerate the iterative process, a relaxation factor ω is incorporated in the solution as

$$h^{n+1} = h^n + \omega^n \Delta h^n \qquad (3.4.3)$$

In the collocation method, the minimum residual method is the process of the minimization of the sum of squares of the residuals at the collocation points. this sum is called the "inner product" and is shown as (R, R). If R_j^n and $R_j^{''}$ are the residuals at the collocation points obtained through the solutions of h^n and $h^n + \Delta h^n$ respectively, we choose ω^n such that (R^{n+1}, R^{n+1}) is minimized. For a linear operator M_{sp},

$$R^{n+1} = R'' - \omega^n (\Delta R) \qquad (3.4.4)$$

where ΔR is determined from

$$\Delta R = R'' - R^n \qquad (3.4.5)$$

The inner product of (3.4.5) can be given as

$$(R^{n+1}, R^{n+1}) = (R'', R^n) - 2\,\omega^n (\Delta R, R'') + \omega^2 (\Delta R, \Delta R) \qquad (3.4.6)$$

The magnitude of (3.4.6) is minimum for a value of the relaxation coefficient

$$\omega^n = \frac{(R'', \Delta R)}{(\Delta R, \Delta R)} \qquad (3.4.7)$$

Using ω^n and (3.4.3), the next guess h^{n+1} is obtained and the process is repeated until the square root of the sum of the residuals decreases no further.

CHAPTER IV

THE SPECTRAL SOLUTION OF EQUATIONS

This chapter presents the salient features of the algorithm of the Spectral Method used in the present work. The algorithm is based on Preconditioned Residual Minimization. The topics covered include the Residual determination, Finite Difference Preconditioning and Preconditioned Residual Minimization. At the end of the chapter, a flow chart of the algorithm used is included. For convenience, the bar has been dropped from the barred variables in Chapter II without changing the nature of the variables.

4.1 Residual Determination

The governing equations are given as below.

$$a_o \frac{\partial h}{\partial t} + b_o\, h \frac{\partial v}{\partial x} + c_o\, v \frac{\partial h}{\partial x} = 0 \qquad (4.1.1a)$$

$$d_o \frac{\partial v}{\partial t} + e_o\, v \frac{\partial v}{\partial x} + f_o \frac{\partial h}{\partial x} - S_r = 0 \qquad (4.1.1b)$$

As mentioned earlier, the spectral scheme is applied by discretizing the temporal derivative with finite difference approximation and the spatial derivatives are estimated using the spectral Chebyshev approximation. Therefore, the residuals in the global field are evaluated for continuity equation (2.2.3a) as

$$r_{cj}^{p+1} \equiv a_o \left[\frac{h^{p+1} - h^p}{\Delta t} \right]_j + \theta \left[b_o h \left(\frac{\partial v}{\partial x} \right) + c_o v \left(\frac{\partial h}{\partial x} \right) \right]_j^{p+1}$$

$$+ (1 - \theta) \left[b_o h \left(\frac{\partial v}{\partial x} \right) + c_o v \left(\frac{\partial h}{\partial x} \right) \right]_j^{p}$$

$$1 \leq j \leq N-1 \qquad (4.1.2a)$$

for momentum equation (2.2.3b) as

$$r_{Mj}^{p+1} \equiv d_o \left[\frac{v^{p+1} - v^p}{\Delta t} \right]_j + \theta \left[e_o v \left(\frac{\partial v}{\partial x} \right) + f_o \frac{\partial h}{\partial x} - S_r \right]_j^{p+1}$$

$$+ (1 - \theta) \left[e_o v \left(\frac{\partial v}{\partial x} \right) + f_o \frac{\partial h}{\partial x} - S_r \right]_j^{p}$$

$$1 \leq j \leq N-1 \qquad (4.1.2b)$$

and at the boundaries

upstream

$$r_1 \equiv q_1 - h_1 v_1 \qquad (4.1.2c)$$

downstream

$$r_N \equiv (x_N - x_{N-1}) h_{N-2} - (x_N - x_{N-2}) h_{N-1} + (x_{N-1} - x_{N-2}) h_N \qquad (4.1.2d)$$

where h^{p+1} and v^{p+1} are the guesses (from the finite difference preconditioner) of variables h and v for time level (p+1), h^p and v^p are the computed values at time p and θ is a weighting factor which varies from 0.5 to 1.

The root mean square (rms) value of the residual or the function to be minimized is defined as the square root of the inner product of the residuals obtained from (4.1.2) i.e.

$$r_{rms} = \left[r_1^2 + r_N^2 + \sum_{j=1}^{N-1} \left(r_{cj}^2 + r_{mj}^2 \right) \right]^{1/2} \qquad (4.1.3)$$

The value of (4.1.3) gets minimized after some iterations and we get a more accurate solution to our governing equations. The whole process of iteration is discussed in the next section.

4.2 Finite Difference Preconditioning

As already mentioned, preconditioning is a good way to accelerate the convergence of iterative schemes designed to solve implicit spectral equations. The approximation matrix resulting from preconditioning should satisfy the following conditions.

(a) the approximation matrix should be a fairly good representation of the original spectral operator matrix M_{ep}.

(b) it should be easy and inexpensive to invert.

The present work uses an implicit first-order finite difference preconditioner which employs forward-differences to discretize the spatial derivatives of the linearized governing equations. The linearization of the governing equation is carried out as follows.

In the governing equation (2.2.3), the dependent variables $\bar{h}$ and $\bar{v}$ are replaced by $(h + \Delta h)$ and $(v + \Delta v)$

respectively, where h and v are some approximation of $\bar{h}$ and $\bar{v}$ obtained from the finite difference implicit scheme and Δh and Δv are the corrections that need to be made to h and v respectively. The equations are expanded in terms of corrections Δh and Δv. The source term S_r is highly non-linear, and is therefore, linearized by using Taylor's expansion. By dropping all second and higher order terms, the linearized equations become

$$a_o \Delta h_t + b_o \Delta v\, h_x + b_o v\, \Delta h_x + c_o \Delta h\, v_x + c_o h\, \Delta v_x = - R_c \qquad (4.2.1a)$$

$$d_o \Delta v_t + e_o \Delta v\, v_x + e_o v\, \Delta v_x + f_o \Delta h_x - \Delta h\, (S_r)_h - \Delta v\, (S_r)_v = - R_M \qquad (4.2.1b)$$

in which

$$(S_r)_h \equiv \frac{\partial S_r}{\partial h} = \frac{4}{3}\, p_o\, n^2\, \frac{v^2}{h^{7/3}} \qquad (4.2.2a)$$

and

$$(S_r)_v \equiv \frac{\partial S_r}{\partial v} = -2\, p_o\, n^2\, \frac{v}{h^{4/3}} \qquad (4.2.2b)$$

And R_c and R_M are the residuals of the original equations for the approximate solution h and v. Subscripts x and t indicate the partial derivatives with respect to x and t respectively.

If the residuals R_c and R_M are known for the current approximations h and v, we can use (4.1.2) to compute the corrections Δh and Δv. We know, of course, only the spectral approximation of R_c and R_M which is computed as given above from

h and v. However , any attempt to solve (4.2.1) directly for the spectral approximation of Δh and Δv will involve solutions of matrix equations that are full and ill-conditioned and computationally very expensive. The approach of finite difference preconditioning is to solve (4.2.1) by obtaining the values of Δh and Δv at the collocation points by solving the finite difference version of (4.2.1) at each collocation points.

Thus the right hand terms of equations (4.2.1) are computed by using (4.1.2) for the present time level values of h and v, and the left hand terms are discretized refer to finite difference form using Preissmann scheme again (But with a different weighting factor, β). After rearranging the corresponding terms, the final system of equations become

$$a_j^c \Delta h_j + b_j^c \Delta v_j + c_j^c \Delta h_{j+1} + d_j^c \Delta v_{j+1} = - R_{cj} \qquad 1 \le j \le N-1 \qquad (4.2.3a)$$

$$a_j^m \Delta h_j + b_j^m \Delta v_j + c_j^m \Delta h_{j+1} + d_j^m \Delta v_{j+1} = - R_{Mj} \qquad 1 \le j \le N-1 \qquad (4.2.3b)$$

and the equations at the boundaries are

$$a_1^u \Delta h_1 + b_1^u \Delta v_1 = - R_1 \qquad (4.2.3c)$$

$$a_{N-2}^d \Delta h_{N-2} + c_{N-1}^d \Delta h_{N-1} + a_N^d \Delta h_N = -R_N \qquad (4.2.3d)$$

The marching techniques used to solve (4.2.3) generates at each marching step, a sparse matrix system of the form as

mentioned earlier (2.3.2.3).

Again this matrix system is solved using a standard library subroutine and the corrections to the solution are thus evaluated. It must be noted that the use of implicit finite difference schemes in the preconditioner ensures its unconditional stability. At the end of an iteration, we obtain the finite difference corrections at the collocation points. Δh_j and Δv_j.

These corrections are multiplied by an acceleration parameter ω and added to h and v to get the new guess of h and v. This entire process is repeated till the process converges, i.e. the rms of the residuals does not decrease any further.

4.3 Preconditioned Residual Minimization

The procedure adopted is as given in Chapter III, with the clarification that the residual R is made up of

(1) the upstream boundary residual R_1

(2) the residuals of the continuity equation R_{cj} at the interior points

(3) the residuals of the momentum equation R_{Mj} at the interior points

(4) the downstream boundary residual R_N.

Therefore the inner product, say, (R, R') is

$$(R, R') = R_1 R_1' + R_N R_N' + \sum_{j=1}^{N-1} R_j R_j' \qquad (4.3.1)$$

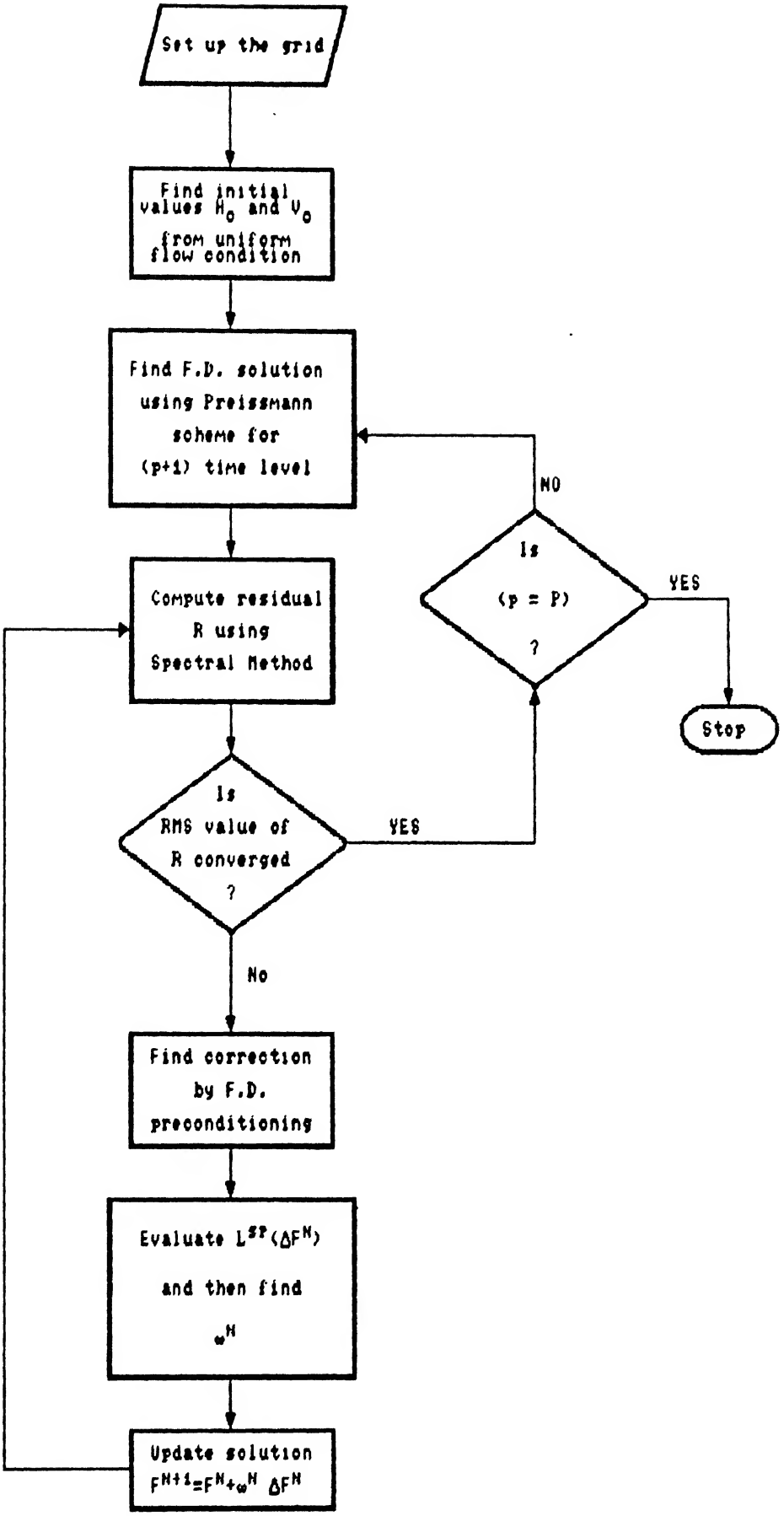

Fig. 4.1 Flow Chart of the Alogrithm

CHAPTER V

RESULTS AND DISCUSSION

In this Chapter, the four-point implicit finite difference and the Chebyshev Collocation spectral methods are used to route a log pearson type III hydrograph through a wide rectangular open-channel. The numerical results so obtained are assessed for their computational accuracy. Two hydrographs are used for this purpose. The peak discharge in both the hydrographs is equal to twenty times the initial steady discharge. However, the peak discharge in the first hydrograph occurs at 72 hours while in the second it occurs at 20 hours. This makes the depth and velocity vary more rapidly in the second case as compared to in the first case. The time at the Centre of Gravity of the hydrograph is taken 1.2 times the time at the peak discharge (t_r=1.2) for both the cases.

The governing partial differential equations do not have an analytical solution for the above boundary condition and in the general case of friction affected flow. This makes it impossible to exactly quantify the error introduced by the numerical scheme. Therefore, in the present study, the finite difference solution using 101 grid points and a computational time step of 10 minutes is taken as "exact solution". The numerical error in any other case is defined as below

$$\% \text{ error} = \frac{F - F_e}{F_e} * 100 \qquad (5.1)$$

where, F represents either the normalized depth or the normalized velocity and the subscript e indicates the "exact" result Equation (5.1) is used to assess the resolution and time stepping errors resulting from the application of finite difference and spectral techniques for routing the flood wave. Three different values of the total number of grid points, N = 41, 21 and 11 are used for evaluating the spatial resolution errors. Two different values of the computational time step, Δt = 10 minutes and 4 hours are used for evaluating the time stepping errors.

5.1 Non-dimensionalization of Equations:

As mentioned, in Chapter II, St. Venant equations have been non-dimensionalized to get the governing equations used in the present study. Using the parameters H_o, V_o and L_o representing the initial uniform flow depth, initial uniform flow velocity and the channel length repectively, it is possible to obtain 12 different sets of normalized equations. However, extensive numerical experimentation has shown that few of these sets give converging numerical results when used for routing the flood hydrograph. Further evaluation of numerical schemes is done only for the best set from the above which is selected by means of the following criteria :

(a) Iteration procedure used for obtaining the spectral solution converges all times and for all computational time steps.

(b) The rms value of residuals obtained from the finite difference solution is generally small.

Coefficients a_o, b_o, c_o, d_o, e_o, f_o, g_o and p_o in the normalized equations (2.2.3) corresponding to all the 12 sets are given in Table 5.1. Remarks based on the earlier mentioned criteria for the "best set" are also included in this table. It can be seen that the set 4 is the "best set" and so it is chosen for further application.

Table 5.1. Coefficients in Normalized St. Venant Equations

Set	1	2	3	4	5
	a_o	b_o	c_o	d_o	e_o
1	$\frac{H_o}{V_o T_o}$	$\frac{H_o}{L_o}$	$\frac{H_o}{L_o}$	$\frac{V_o}{g\ T_o}$	$\frac{V_o^2}{g\ L_o}$
2	$\frac{H_o}{V_o T_o}$	$\frac{H_o}{L_o}$	$\frac{H_o}{L_o}$	1.0	$\frac{V_o T_o}{L_o}$
3	$\frac{H_o}{V_o T_o}$	$\frac{H_o}{L_o}$	$\frac{H_o}{L_o}$	$\frac{V_o\ L_o}{g\ H_o\ T_o}$	$\frac{V_o^2}{g\ H_o}$
4	1.0	$\frac{V_o T_o}{L_o}$	$\frac{V_o T_o}{L_o}$	$\frac{V_o}{g\ T_o}$	$\frac{V_o^2}{g\ L_o}$
5	1.0	$\frac{V_o T_o}{L_o}$	$\frac{V_o T_o}{L_o}$	1.0	$\frac{V_o T_o}{L_o}$
6	1.0	$\frac{V_o T_o}{L_o}$	$\frac{V_o T_o}{L_o}$	$\frac{L_o\ V_o}{g\ H_o\ T_o}$	$\frac{V_o^2}{g\ H_o}$
7	$\frac{L_o}{V_o\ T_o}$	1.0	1.0	$\frac{V_o}{g\ T_o}$	$\frac{V_o^2}{g\ L_o}$
8	$\frac{L_o}{V_o\ T_o}$	1.0	1.0	1.0	$\frac{V_o T_o}{L_o}$
9	$\frac{L_o}{V_o\ T_o}$	1.0	1.0	$\frac{L_o\ V_o}{g\ H_o\ T_o}$	$\frac{V_o^2}{g\ H_o}$
10	$\frac{H_o}{V_o T_o}$	$\frac{H_o}{L_o}$	$\frac{H_o}{L_o}$	$\frac{L_o}{V_o\ T_o}$	1.0
11	1.0	$\frac{V_o T_o}{L_o}$	$\frac{V_o T_o}{L_o}$	$\frac{L_o}{V_o\ T_o}$	1.0
12	$\frac{L_o}{V_o\ T_o}$	1.0	1.0	$\frac{L_o}{V_o\ T_o}$	1.0

(continued to next page)

(continued from previous page)

Set	6	7	8	9
	f_o	g_o	h_o	REMARKS
1	$\frac{H_o}{L_o}$	1.0	$V_o^2/H_o^{4/3}$	Does not converge
2	$\frac{g\ H_o\ T_o}{V_o\ L_o}$	$\frac{g\ T_o}{V_o}$	$V_o^2/H_o^{4/3}$	High residuals
3	1.0	$\frac{L_o}{H_o}$	$V_o^2/H_o^{4/3}$	High residuals
4	$\frac{H_o}{L_o}$	1.0	$V_o^2/H_o^{4/3}$	Lowest Residuals
5	$\frac{g\ H_o\ T_o}{V_o\ L_o}$	$\frac{g\ T_o}{V_o}$	$V_o^2/H_o^{4/3}$	High residuals
6	1.0	$\frac{L_o}{H_o}$	$V_o^2/H_o^{4/3}$	Residuals higher than that of Set 4
7	$\frac{H_o}{L_o}$	1.0	$V_o^2/H_o^{4/3}$	Residuals same as that of Set 5
8	$\frac{g\ H_o\ T_o}{V_o\ L_o}$	$\frac{g\ T_o}{V_o}$	$V_o^2/H_o^{4/3}$	High residuals
9	1.0	$\frac{L_o}{H_o}$	$V_o^2/H_o^{4/3}$	Residuals same as that of Set 5
10	$g\ H_o/V_o^2$	$g\ H_o/V_o^2$	$V_o^2/H_o^{4/3}$	Very high residuals & does not converge
11	$g\ H_o/V_o^2$	$g\ H_o/V_o^2$	$V_o^2/H_o^{4/3}$	Very high residuals & does not converge
12	$g\ H_o/V_o^2$	$g\ H_o/V_o^2$	$V_o^2/H_o^{4/3}$	Very high residuals & does not converge

5.2 Weighting Parameters α, β, and θ

The finite difference method presented in Chapter II and the spectral method using the Chebysev Collocation technique presented in Chapters III and IV uses three weighting parameters α, β, and θ. These parameters are used in order to give a proper weightage to the solution towards the unknown time level (p+1). α is the weighting coefficient used while finding the initial solution by the Preissmann Scheme. θ is the weighting coefficient

in the Chebysev Collocation technique used for finding the residuals of either the finite difference solution or the residuals during the iteration stage of spectral method. β is the weighting coefficient in the finite difference preconditioning part of the spectral method. It should be noted that $\alpha = \theta = 0.5$ result in a second-order accuracy in time and $\alpha = \theta = 1.0$ result in a completely implicit first-order accurate method. Exhaustive numerical experimentation during the preliminary stage of model development has indicated that $\alpha = 0.66$, $\beta = 0.85$ and $\theta = 1.0$ result in good numerical convergence and the lowest residuals. It proved to be very difficult to obtain convergent results with $\theta = 0.5$. It can be seen from the above discussion that the finite difference method applied in the present study, is almost second-order accurate ($\alpha = 0.66$) while the spectral method is only first-order accurate ($\theta = 1.0$) as far as time discretization is concerned. It should be remembered here that the spectral method as applied in the present study, achieves spectral accuracy only in space while it uses a finite difference time stepping.

5.3 Results for equations without Source Term

As mentioned in Chapter II, the right hand side of equation (2.2.3b) is termed as the Source term of the momentum equation. The governing partial difference equations are strictly hyperbolic only when this term is equal to zero. On the other hand, in many natural flow situations, the source term is more dominant than the other terms in the momentum equation. In such cases, it can be shown that the equations are of diffusion type

when the acceleration terms in the momentum equation are neglected. It can also be seen that the source term which includes the frictional effects (Eq. 2.2.4) is highly non-linear. Therefore, difficulties are encountered while including the frictional effects in the numerical models. This is especially so, as experienced during the course of this study, when one is interested in increasing the order of accuracy of numerical schemes. Therefore, the spectral technique for solving the St. Venant equations has been developed in two stages. In the first stage, it has been assumed that the channel is almost horizontal and frictionless, results for which are discussed in the present section. In the second stage of development, an attempt has been made to include the frictional and channel slope effects into the model. Results for the above case are discussed in the next section.

The numerical results, i.e. the depth and velocity values, are obtained at all the grid points as functions of time. However, only the results for channel mid-section are presented below. Similar trend is observed at all the other points. Figures 5.1a and 5.1b show the normalized depth and normalized velocity as function of normalized time at the channel mid-section for the first hydrograph. These results, obtained using the F.D scheme with 101 grid points and Δt = 10 minutes, are taken as "exact solutions". In the same way, Figures 5.2a and 5.2b show the "exact solutions" for depth and velocity at the channel mid-section for the second hydrograph. It can be seen that although the peak depth is approximately the same in both cases,

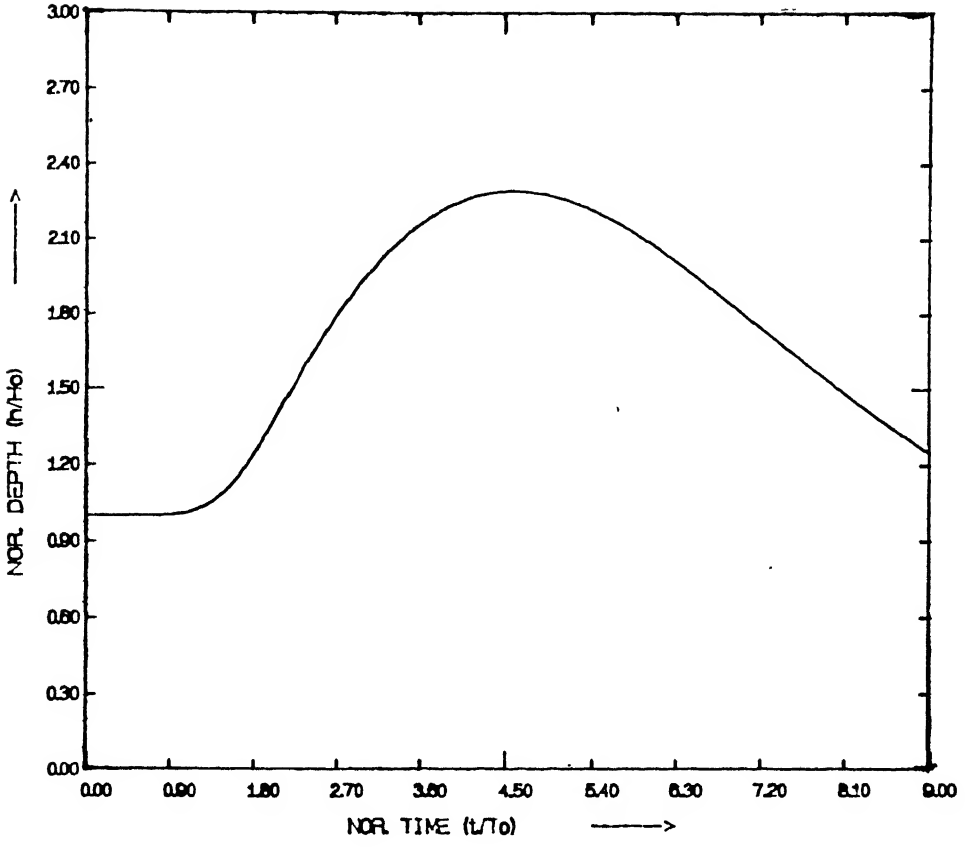

(a) Normalized Depth vs Normalized Time

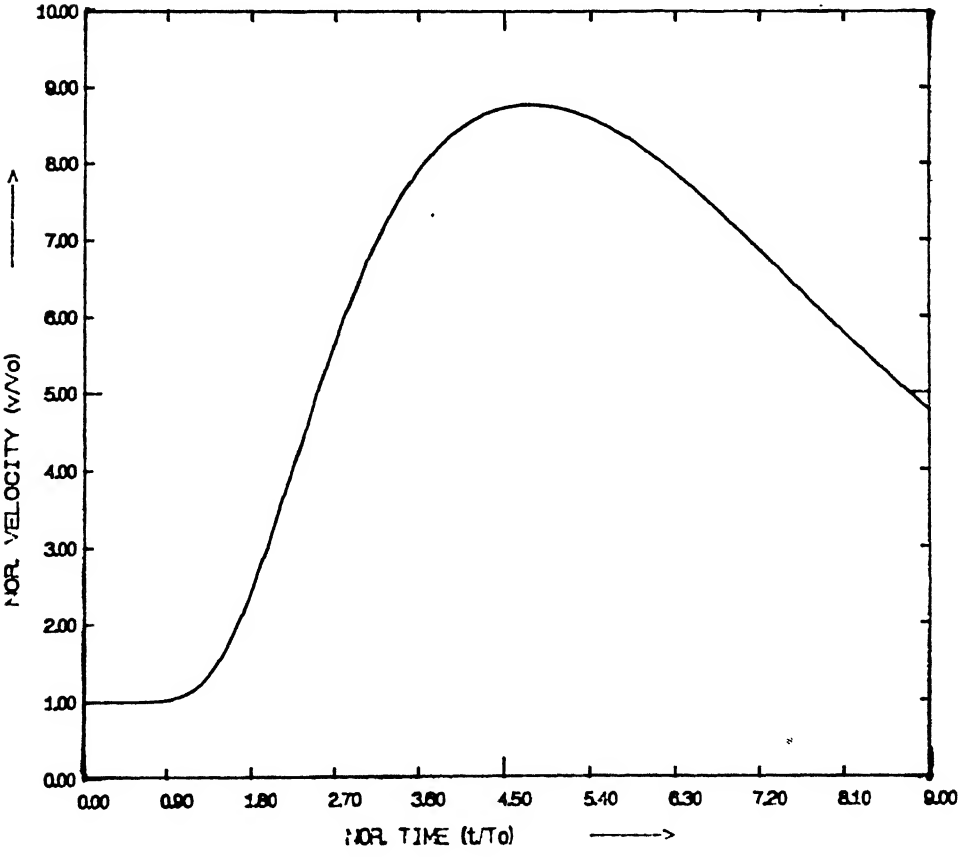

(b) Normalized Velocity vs Normalised Time

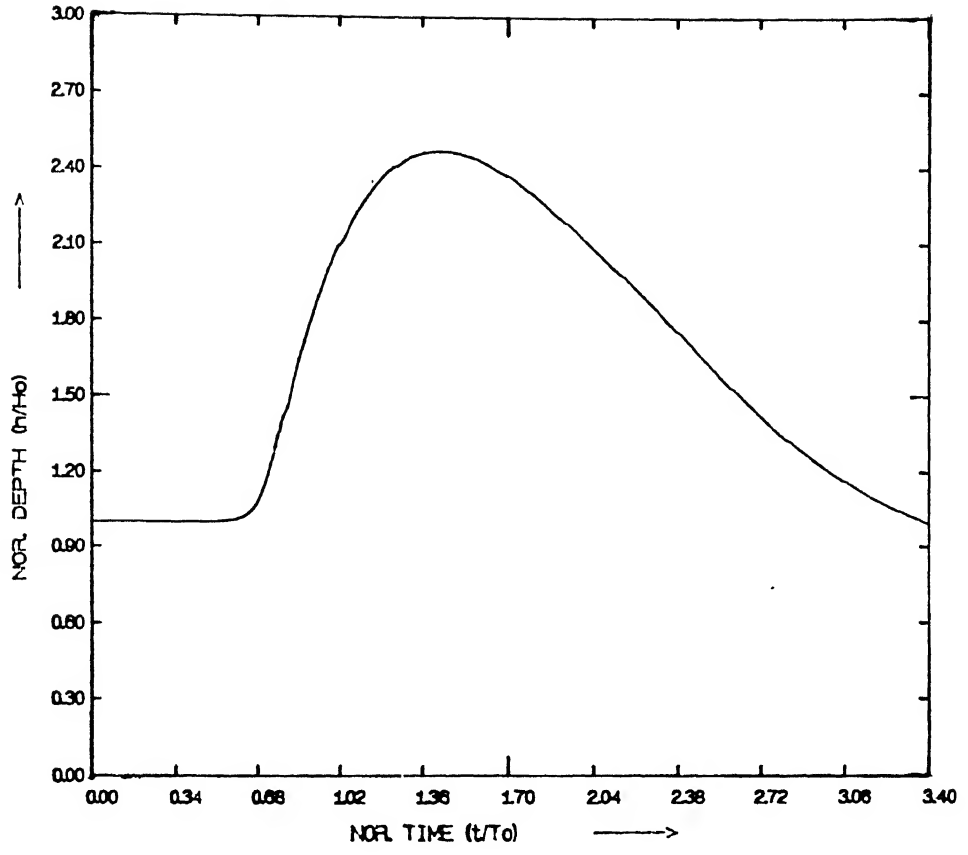

(a) Normalized Depth vs Normalized Time

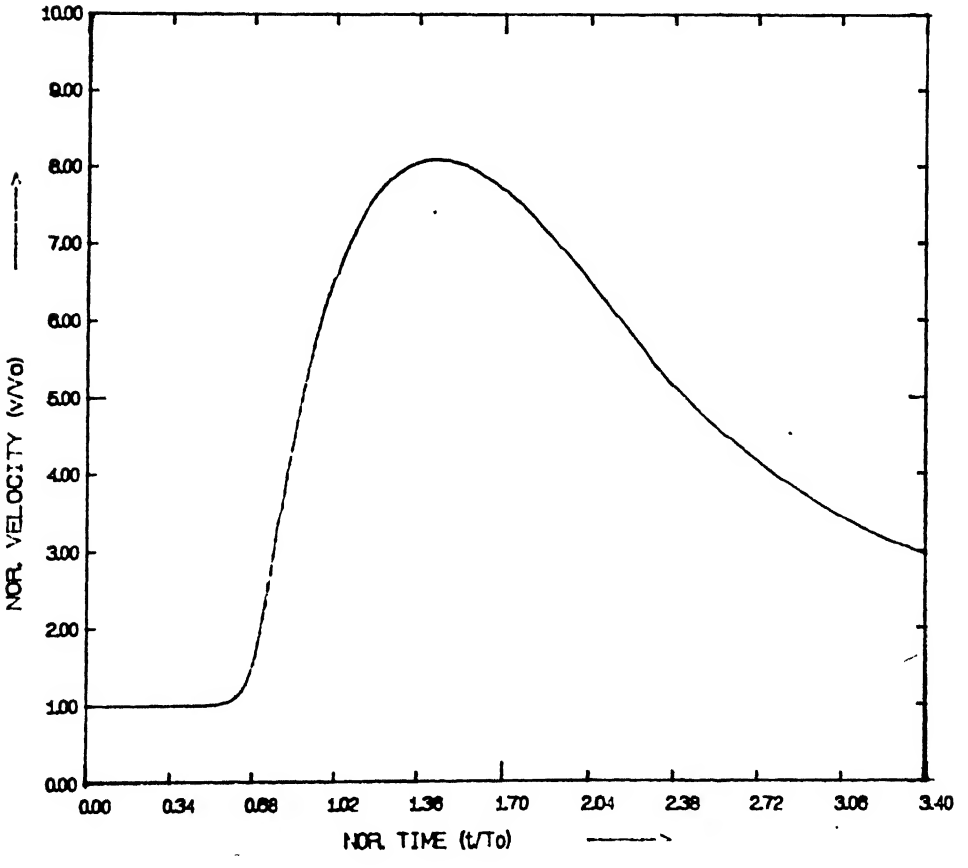

(b) Normalized Velocity vs Normalised Time

Fig. 5.2 "Exact Solution" for Hydrograph-2, Δt=10 minutes

it is attained at a much faster rate in the case of second hydrograph.

In order to study the behaviour of spatial resolution errors, computer runs were made using the same Δt (= 10 minutes) as before, but with a reduced number of grid points, N = 41, 21 and 11. Figures 5.3a and 5.3b show the % error in depth computation (calculated using Eq. 5.1) as a function of time for spectral and finite difference methods respectively. It is obvious from these figures that in both methods the results converge to "exact solution" as the number of grid points are increased. However, looking the other way round, it can be observed that the finite difference solution (Fig. 5.3b) deteriorates faster than the spectral solution (Fig 5.3a) as the number of grid points is decreased. This is expected since spectral techniques theoretically give "infinite-order" accuracy and in the present case, we are minimizing the time stepping errors by taking a very low value of Δt. Similar trend is observed when % error in velocity computation, for first hydrograph, is plotted (Figs. 5.4a and 5.4b) as a function of time.

Figures 5.5a and 5.5b show the % error in depth computation as a function of time for spectral and finite difference methods respectively for the second hydrograph. Here, again the finite difference solution, in general, deteriorates faster than the spectral solution as the number of nodes (N) is decreased. However, just before the occurrence of peak depth, the error in the spectral solution (4.5%) is slightly more than the error in the finite difference solution (3.2%). This is due to the

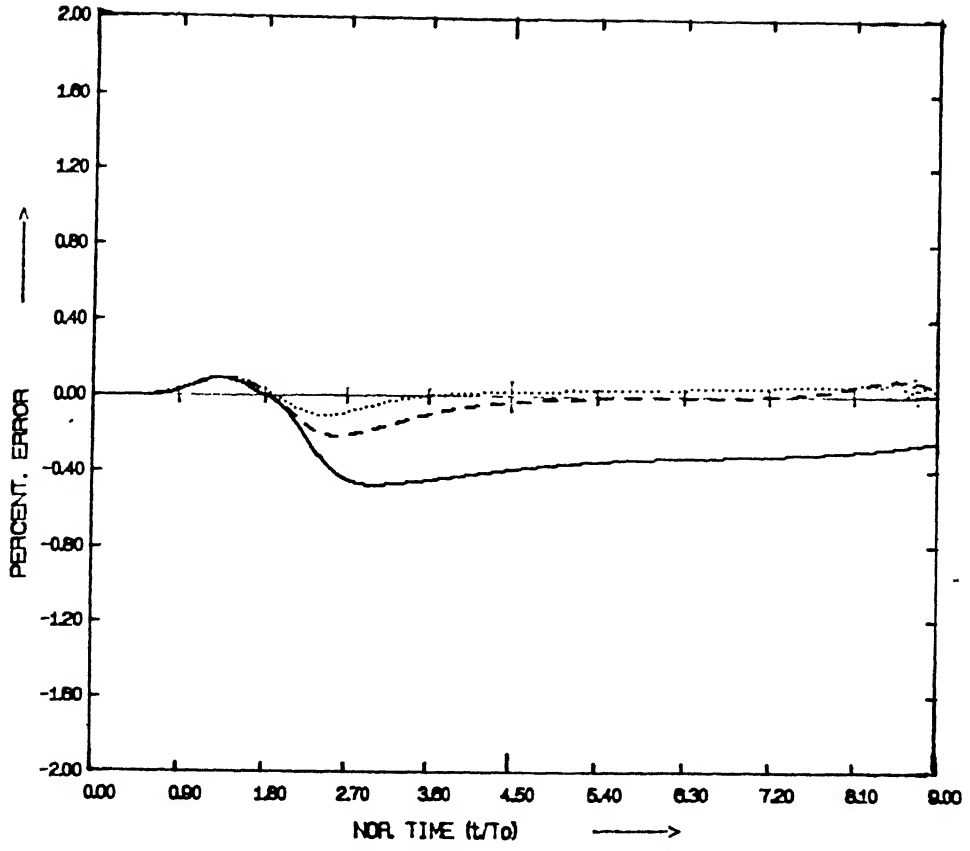

(a) Spectral Solution

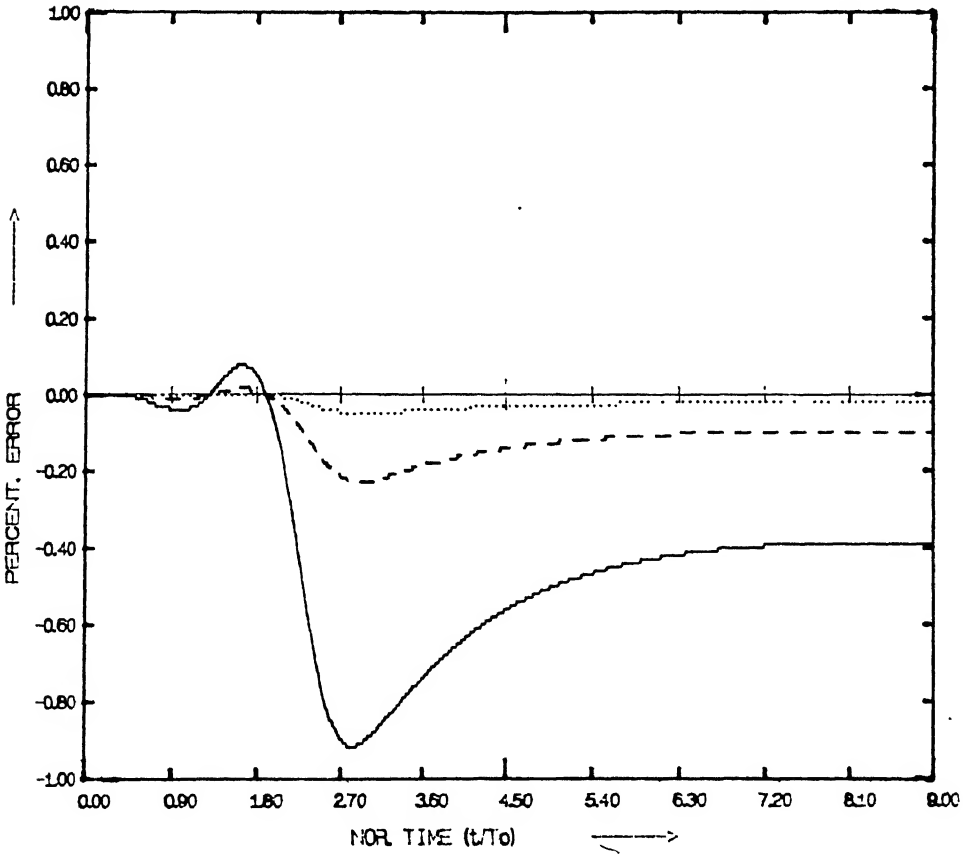

(b) Finite Difference Solution

Fig. 5.3 Spatial Resolution Error in Depth Computation, Hydrograph-1, Δt=10 minutes

——— N=11 - - - N=21 ····· N=41

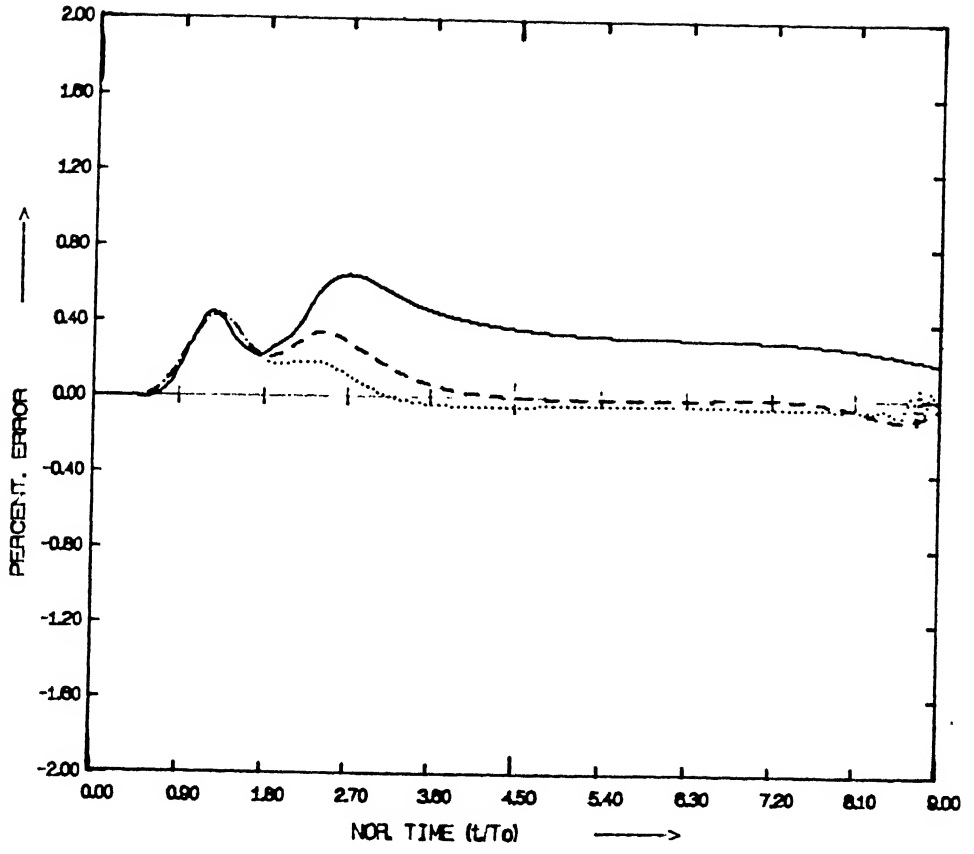

(a) Spectral Solution

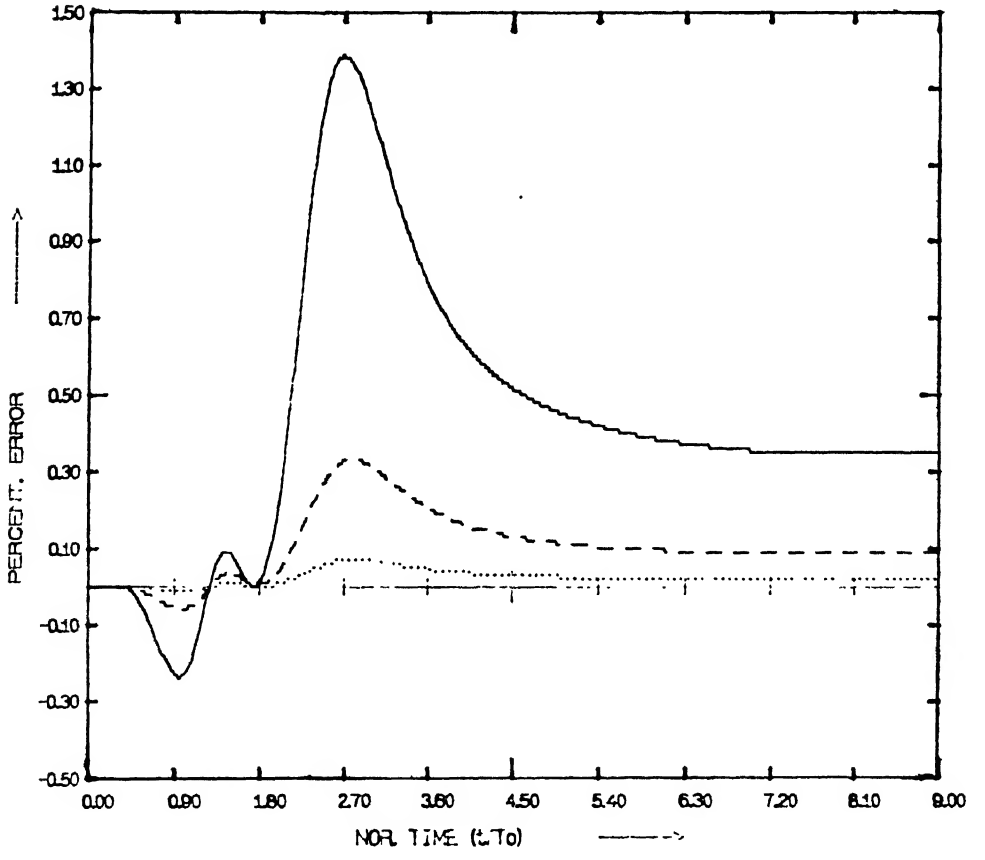

(b) Finite Difference Solution

Fig. 5.4 Spatial Resolution Error in Velocity Computation, Hydrograph-1, Δt=10 minutes

——— N=11 - - - N=21 ····· N=41

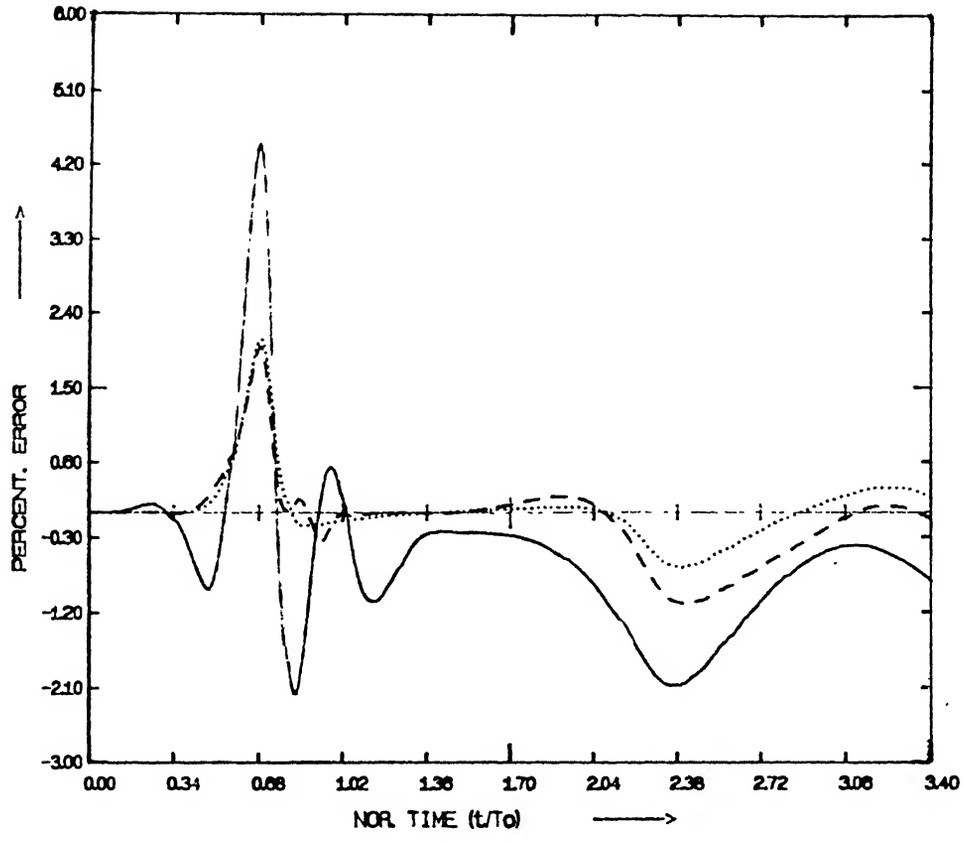

(a) Spectral Solution

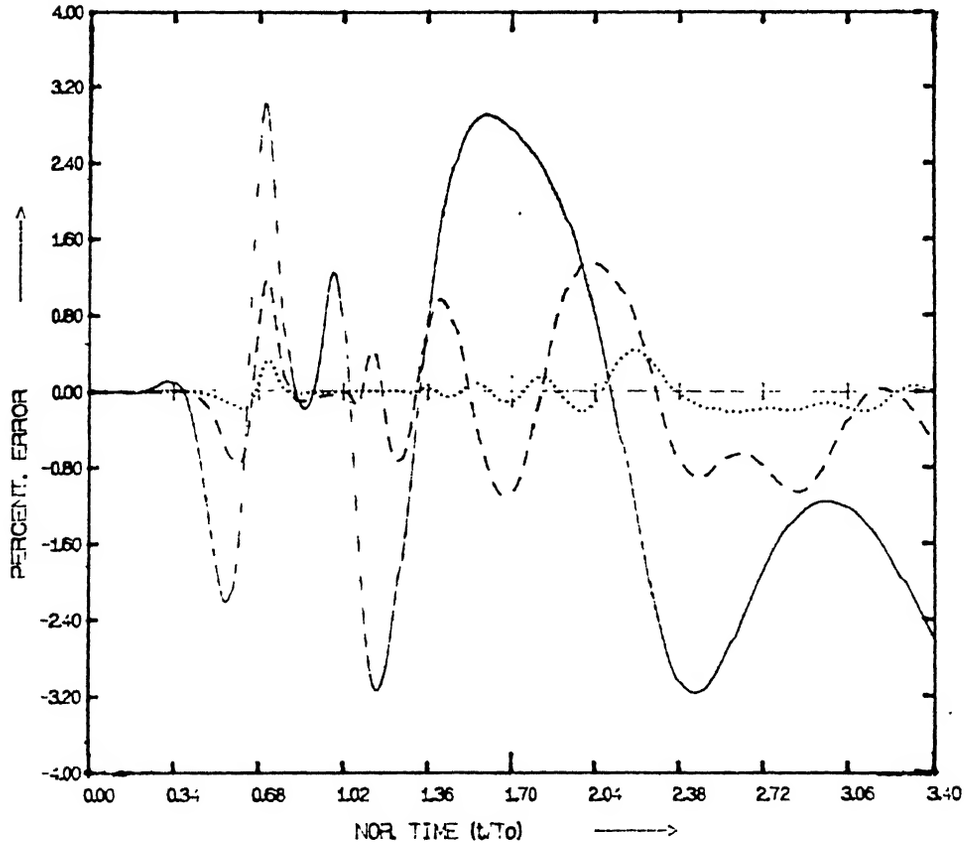

(b) Finite Difference Solution

Fig. 5.5 Spatial Resolution Error in Depth Computation, Hydrograph-2, Δt=10 minutes

——— N=11 - - - N=21 ····· N=41

fact that the finite difference scheme is almost second-order accurate in time while the spectral method is first-order accurate. It should be noted that the second hydrograph represents a faster rising flood and therefore, the time stepping errors are more predominant.

The domenance of time-stepping errors over the spatial resolution errors becomes more accentuated when the computational time step is increased. Figures 5.6a and 5.6b show the error variation in the depth computation for the first hydrograph when the computational time step, Δt equals to four hours. It should be mentioned that this time step, though large is not unrealistically so, for the given hydrographs. The error in the spectral solution (Fig 5.6a) is in the range of 2% whereas the error in the finite difference solution (Fig 5.6b) is only about 1%. This trend becomes more clear when computations are made for the faster rising second hydrograph. The error in the spectral solution is as much as 15% (Fig 5.7a) while the error in the finite difference solution (Fig 5.7b) is only in the range of 5%. This, clearly, indicates the dominance of time stepping errors for the cases studied here.

5.4 Results for Equations with Source Term

In this section, the results obtained from the application of complete St. Venant equations including the source terms for routing a flood hydrograph are presented. Results for only the first hydrograph are discussed. Similar trend was observed when computations were made for the second hydrograph.

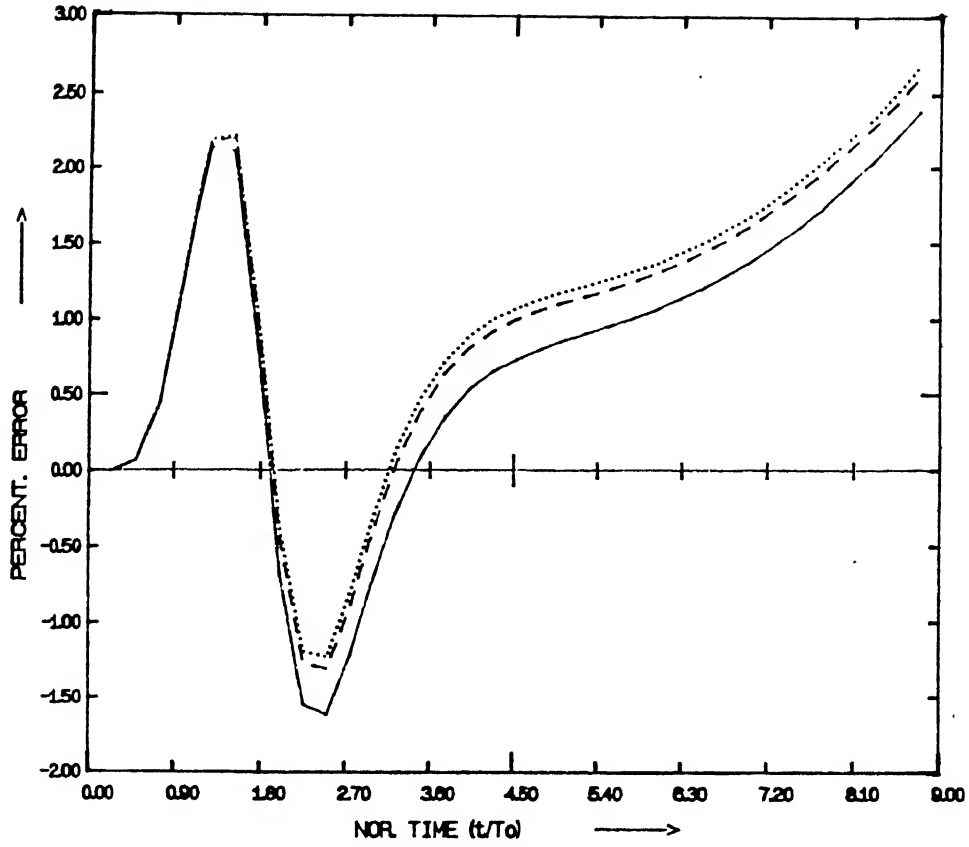

(a) Spectral Solution

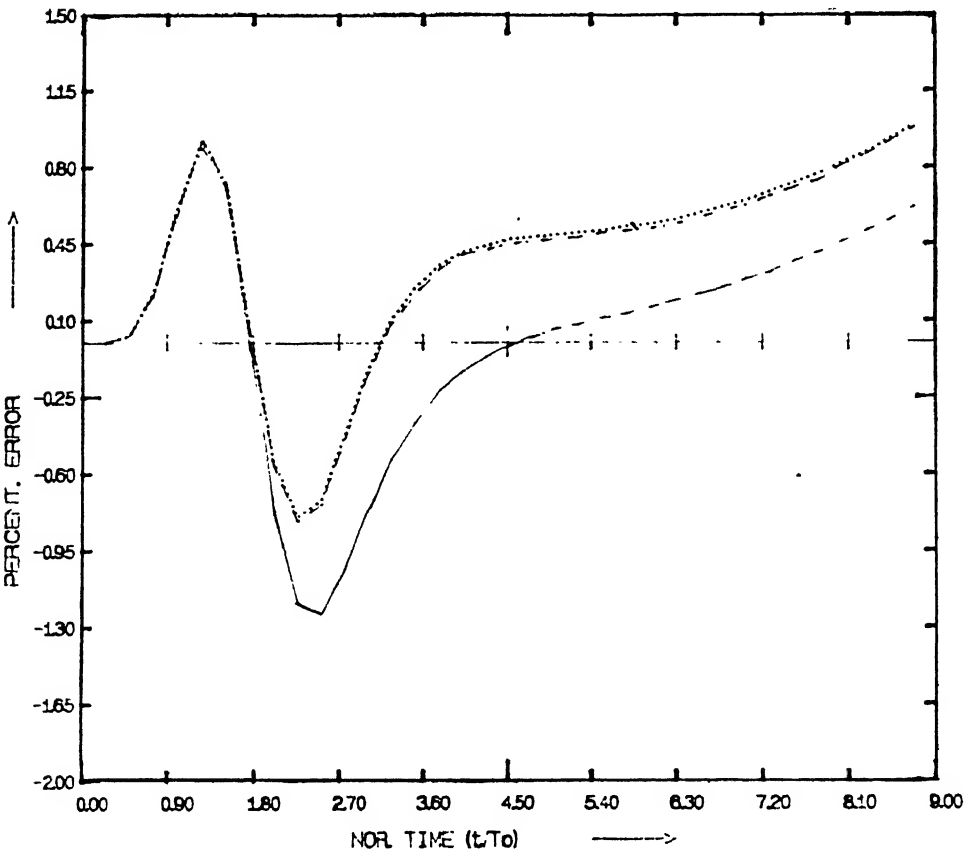

(b) Finite Difference Solution

Fig. 5.6 Time Stepping Error in Depth Computation, Hydrograph-1, Δt=4 hours

——— N=11 - - - N=21 ····· N=41

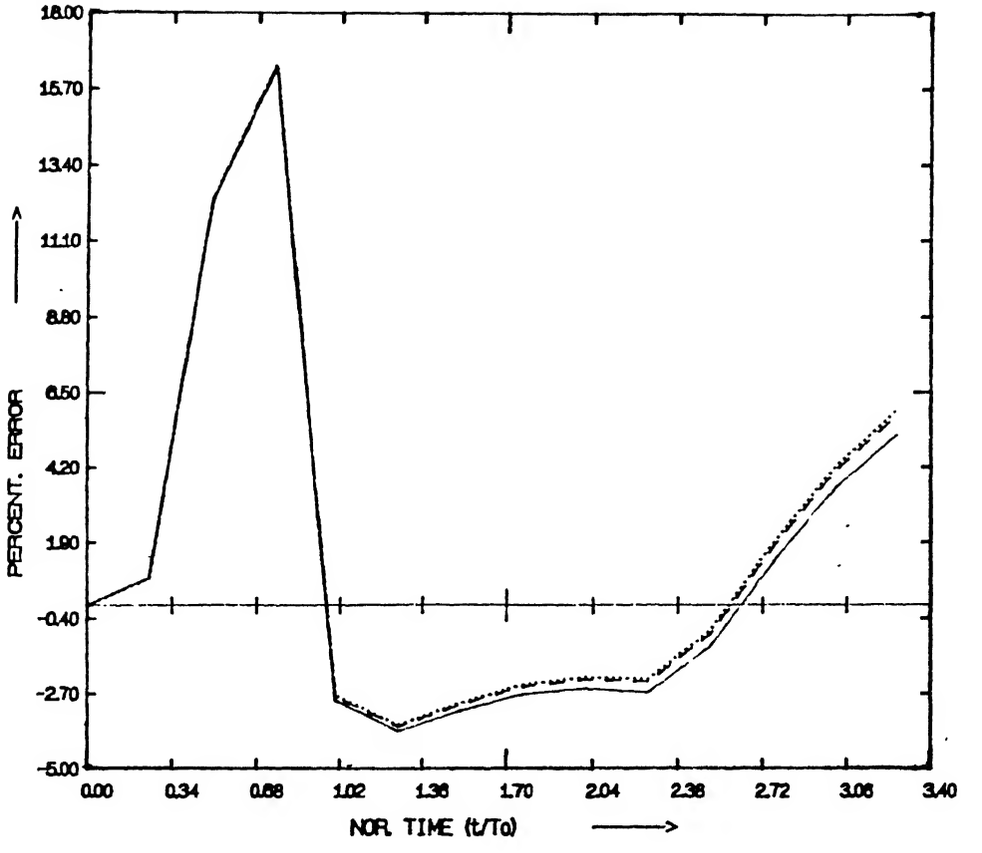

(a) Spectral Solution

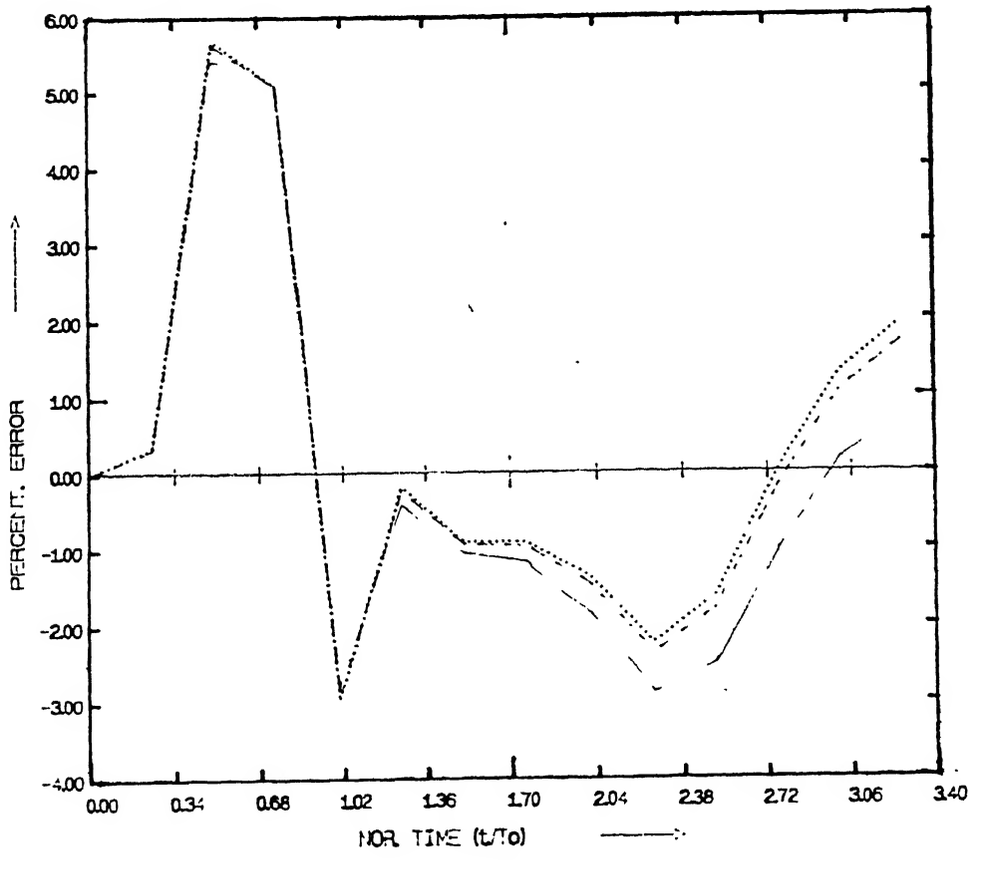

(b) Finite Difference Solution

Fig. 5.7 Time Stepping Error in Depth Computation, Hydrograph-2, Δt=4 hours

——— N=11 - - - N=21 ..... N=41

Fig 5.8 shows the normalized depth at the channel mid-section obtained using the Preissmann scheme with 101 grid points and Δt equal to 10 minutes. This is taken as the "exact solution" for further comparisons. It should be mentioned that the hydrograph used in this study is exactly the same as the one used by Cooley and Moin (1976) in their finite-element model. The solution is shown in Fig 5.8 is essentially the same as obtained by them.

Figures 5.9a and 5.9b show the percentage error in depth computation for spectral and finite difference methods, respectively, when the number of grid points is reduced. Three different N values equal to 41, 21 and 11 are used for studying the spatial resolution errors. It can be observed that error in peak depth estimation (normalized time = 4.5) is insignificant even when as few as 11 nodes are used. This is true for both spectral and finite difference solutions. The numerical error occurs only in the rising limb of the hydrograph. It is observed that the errors in the spectral solutions (fig 5.9a) are of the same order of magnitude as the errors in finite difference solutions (Fig 5.9b). It should be noted here that the frictional effects inhibit the free movement of hydrograph down the channel, thereby resulting in higher flow depths. For example, the peak normalized depth is approximately equal to 2.3 when the source terms are not included and it is approximately equal to 6 when the source terms are included. However, the time of occurrence of of peak depth is almost same in both the cases. This indicates that the time variation in depth is more pronounced when the same source terms are included. As a consequence, the time-stepping

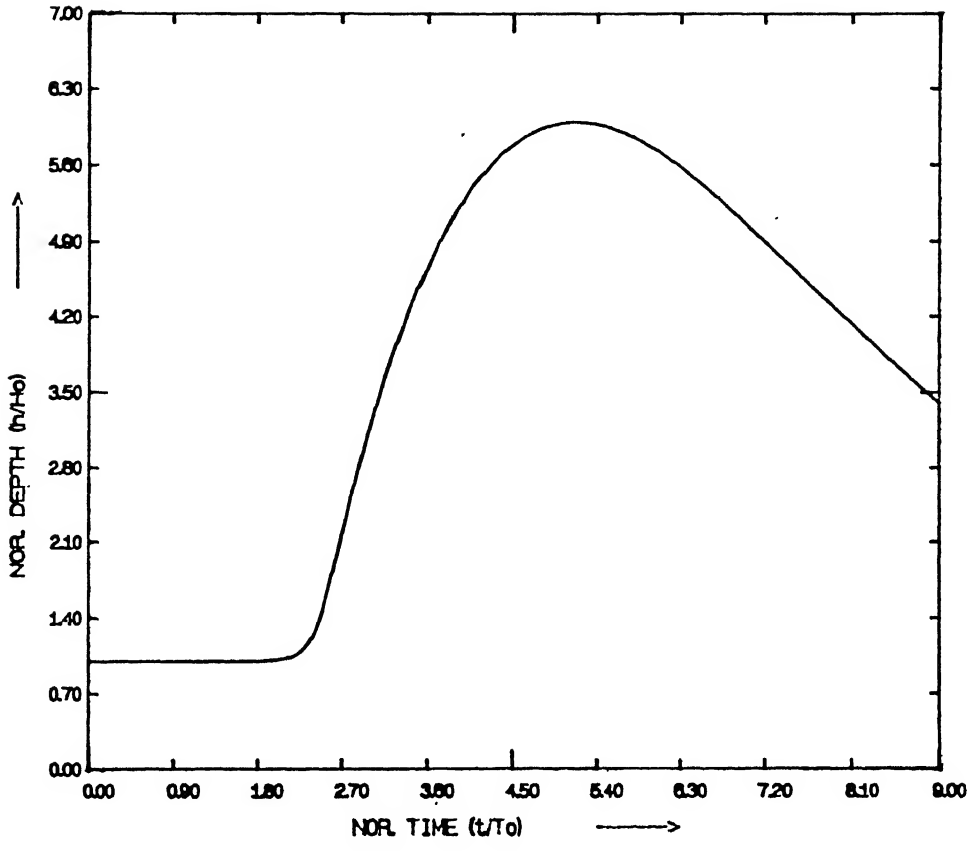

Fig. 5.8 "Exact Solution" for Hydrograph-1, Δt=10 minutes Source Term Included

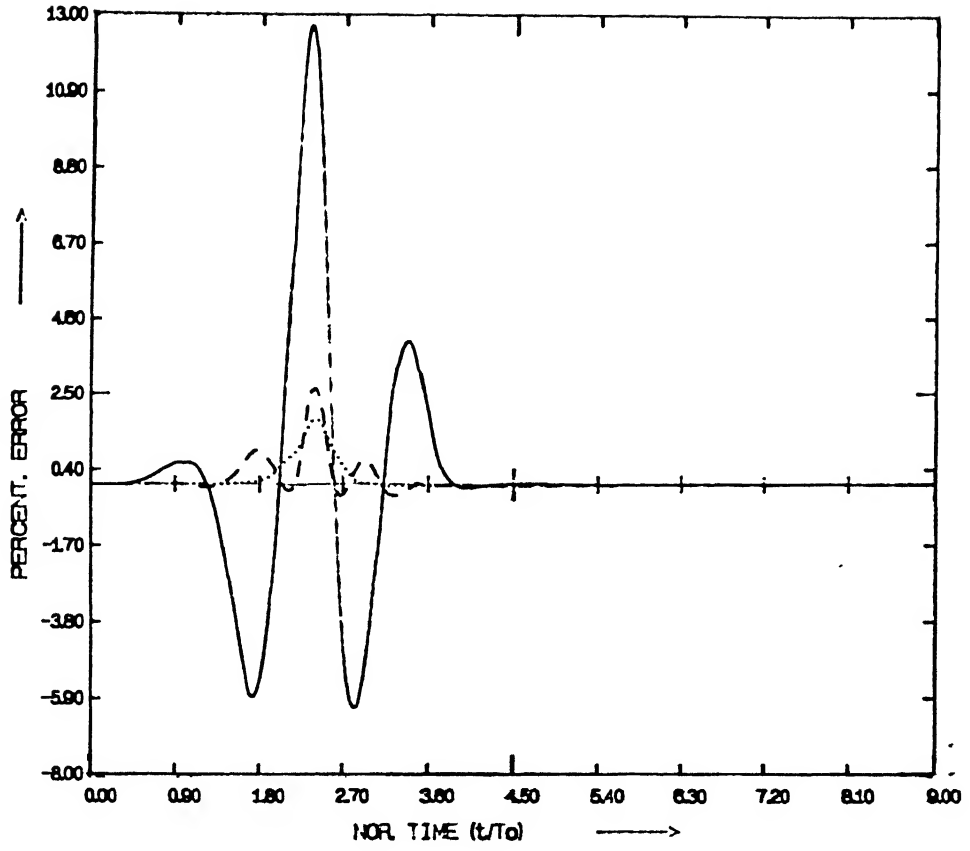

(a) Spectral Solution

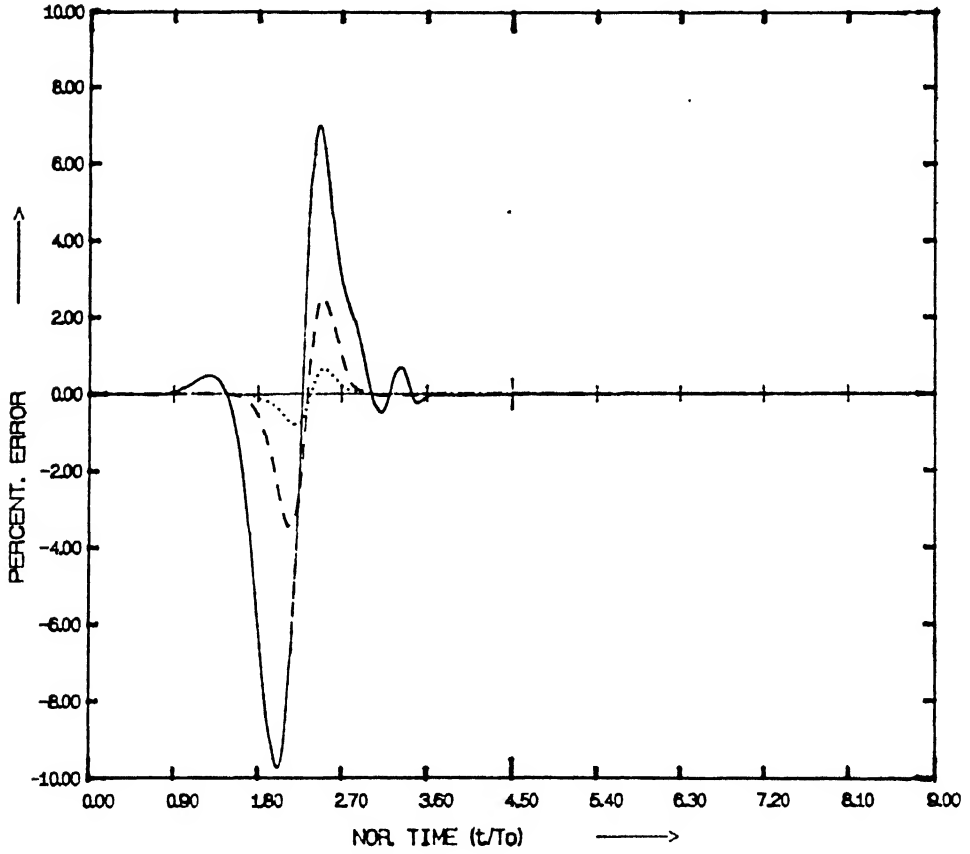

(b) Finite Difference Solution

Fig. 5.9 Spatial Resolution Error for Hydrograph-1, Source Term Included

——— N=11 - - - N=21 ..... N=41

procedure becomes more important than the spatial resolutions. Therefore, the spectral method which is only first-order accurate in time does not give significantly better results than those obtained using the second-order time-accurate finite difference scheme. This conclusion is reinforced by the results obtained for the second hydrograph (not shown here).

The dominance of time stepping errors is demonstrated more dramatically when the computational time step, Δt = 4 hours. Figure 5.10 shows the error in depth computation as a function of time when Δt = 4 hours. As before, error in the peak depth estimation (normalized time = 4.5) is insignificant for both spectral and finite difference solutions. However, the error in the rising limb of the hydrograph is as much as 39% when spectral method is used as compared to an error of 15% in the finite difference solution. The dominance of time-stepping errors is clearly demonstrated by the fact that there is no improvement in the solution even when the number of grid points is increased from N = 11 to N = 41.

5.5 Computational Time

The total number of operations per time-step envolved in finite difference method and in spectral method is approximately equal to $30\ N^2+168\ N$ and $60\ N^2+350\ N$ respectively.

The ratio of the C.P.U. time per iteration taken by the finite difference method to that taken by the spectral method is approximately 4.0.

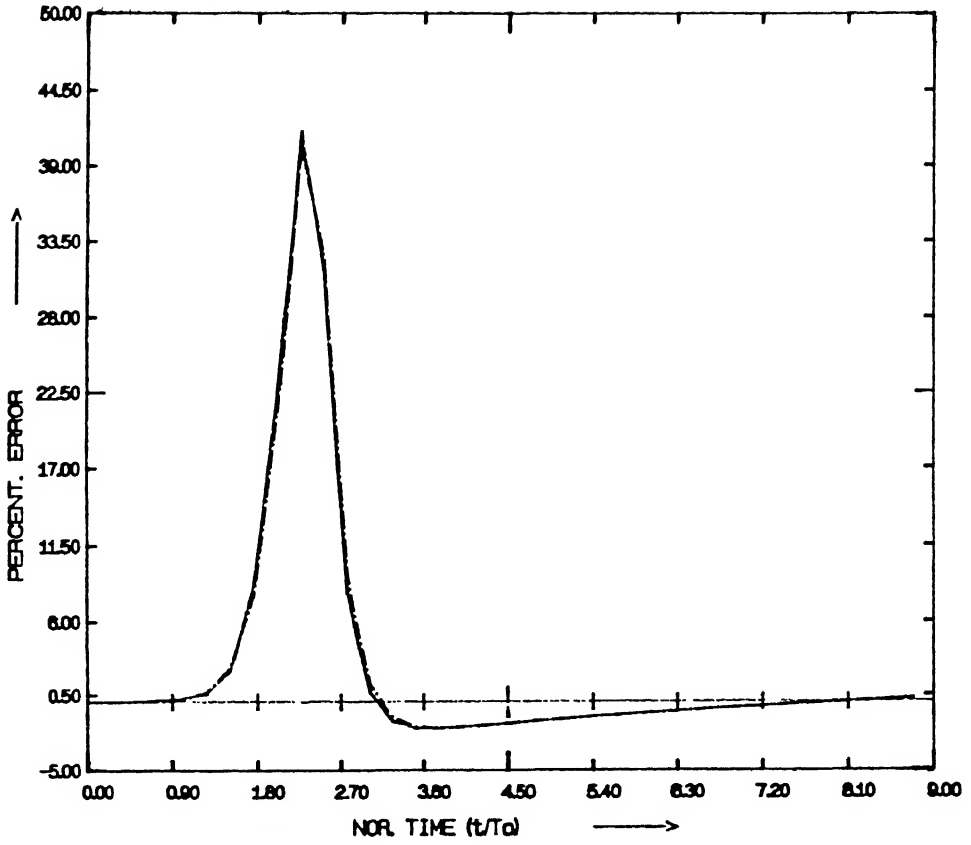

(a) Spectral Solution

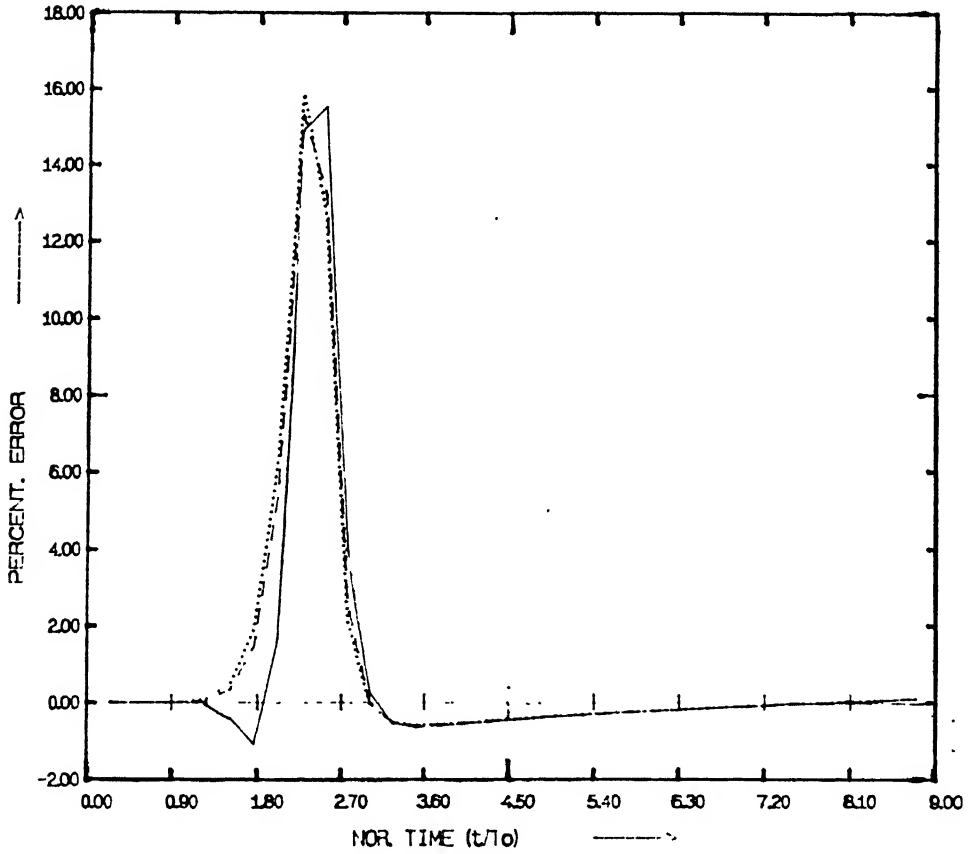

(b) Finite Difference Solution

Fig. 5.10 Time Stepping Error for Hydrograph-1, Source Term Included

——— N=11 - - - N=21 ..... N=41

5.6 Conclusions

From the above discussion, it can be concluded that a spectral method which achieves spectral accuracy only in Space is not good for solving unsteady shallow-water flow equations. A finite difference scheme which is only first-order accurate in space, but second-order accurate in time gives much better results with less amount of computational effort. Therefore, future work in this area should concentrate on developing fully spectral methods which achieve spectral accuracy in time also.

CHAPTER VI

SUMMARY

This investigation presents a Spectral Method for solving the one-dimensional shallow-water wave equations. The spectral method is based on the Chebyshev Collocation technique and a first-order finite difference time stepping. The method developed in this study is applied to route a log-pearson type III hydrograph through a wide rectangular channel. The spectral solutions are compared with the solutions obtained using the Preissmann finite difference scheme which is first-order accurate in space and second-order accurate in time. An error analysis is made through a parametric study. Following are the conclusion obtained from this study:

(1) Both the spectral and the finite difference schemes do not introduce significant errors as far as peak depth simulation is concerned. However, the numerical results show significant errors in the rising limb of the hydrograph. This is especially true when large computational time step and few grid points are used.

(2) Finite difference solution deteriorates faster than the spectral solution when the number of grid points is reduced while keeping the computational time step small i.e. keeping time stepping errors low.

(3) The spectral solution is worse than the finite difference solution whenever the time stepping errors

are predominant aswhen the hydrograph has a fast rising limb. Time stepping errors are also significant when the effect of friction is predominant.

It is suggested that the future work in this area should concentrate on developing fully spectral methods which achieve spectral accuracy in both space and time. The present model may also be modified so that it can be applied for diffusion routing in a more efficient manner. A significant application for the spectral methods would be in the area of sediment transport modeling where aggradation and degradation of channel beds occur over long reaches and over long periods of time.

REFERENCES

1. Abbott, M.B. and Ionescu, F., (1967), "On the Numerical Computation of Nearly Horizontal Flows," *Jour. of Hyd. Res.*, V.5, No.2, pp.97-117.

2. Abbott, M.B., (1979), *Computational Hydraulics*; Elements of the Theory of Free Surface Flows, Pitman Publishing Limited, London.

3. Amein, M., (1966), "Streamflow Routing on Computer by Characteristics," *Water Res. Res.*, V.2, No.1, First quarter, pp.123-130.

4. Amein, M. and Fang, C.S., (1970), "Implicit Flood Routing in Natural Channels," *Jour. of Hyd. Div.*, A.S.C.E., V.96, No.HY12, December, pp.2481-2500. Discussion ; V.97, No.HY7, July, 1971, pp.1156-1159; No.HY9, September, 1971, pp.1552-1555.

5. Baltzer, R.A. and Lai, C., (1968), "Computer Simulation of Unsteady Flows in Waterways," *Jour. of Hyd. Div.*, A.S.C.E., V.94, No.HY4, July, pp.1083-1117.

6. Beam, R.M. and Warming, R.F., (1976), "An Implicit Finite Difference Algorithm for Hyperbolic Systems in Conservation Law Form," *Jour. of Computational Physics*, 22, pp.87-110.

7. Canuto, C., Hussaini, M.Y., Quarteroni, A. and Zang, T.A., (1987), *Spectral Methods in Fluid Dynamics*, Springer-Verlag Publications.

8. Chaudhry, Y.M. and Contractar, D.N., (1973), "Application of Implict Method to surges in Channels," *Water Res. Res.*, V.9, No.6, pp.1605-1612.

9. Chaudhry, M.H., (1987), *Applied Hydraulic Transients*, Nostrand Reinhold Company, New York.

10. Chen, Y.H. and Simons, D.B., (1975), "Mathematical Modeling of Alluvial Channels," *Proc. Symp. on Modeling Technique*, A.S.C.E., San Francisco, V.1, pp.466-483.

11. Cooley, R.L. and Moin, S.A., (1976), "Finite Element Solution of St. Venant Equations," *Jour. of Hyd. Div.*, A.S.C.E., V.102 No. HY6, June, pp.759-775.

12. Cunge, J.A., Holly, F.M. and Verwey, A., (1980), *Practical Aspects of Computational River Hydraulics*, Pitman Publications, 1020 Plain Street, Marsh Field, Massachusetts 0 2050.

13. Dressler, R.F., (1952), "Hydraulic Resistance Effect upon the Dam-Break Functions," *Jour. of Research*, National Bureau of Standards, V.49, No.3, September, pp.217-225.

14. Dronkers, J.J., (1969), "Tidal Computations for Rivers, Coastal Areas and Seas," *Jour. of Hyd. Div.*, A.S.C.E., V.95, No.HY1, January, pp.29-77.

15. Elaisen, E., et al., (1970), "On a Numerical Method for Integration of the Hydrodynamical Equations with a Spectral Representation of the Horizontal Fields," Rep. No.2 (Institute for Teoretisk Meteorologi, Univ. Copenhagen)

16. Ellis, J., (1970), "Unsteady Flow in Channel of Variable Cross-Section," *Jour. of Hyd. Div.*, A.S.C.E., V.96, No.HY10, October, pp.1927-1945.

17. Fennema, R.J. and Chaudhry, M.H., (1986), "Explicit Numerical Schemes for Unsteady Free-Surface Flows with Socks," *Water Res. Res.*, V.22, No.13, pp.1923-1930.

18. Fennema, R.J. and Chaudhry, M.H., (1990), "Numerical Solution of Two-Dimensional Transient Free-Surface Flows," *Jour. of Hyd. Eng.*, V.116, August, pp.1013-1034.

19. Fread, D.L., (1973), "Technique for Implicit Dynamic Routing in Rivers with Tributaries," *Water Res. Res.*, V.9, No.4, pp.918-926.

20. Fread, D.L., (1974), "Numerical Properties of Implicit Four-Point Finite Difference Equations of Unsteady Flow," *NOAA Tech. Memo. NWS HYDRO-18*, U.S. Dept. of Commerce, National Weather Service, Silver Spring, Maryland.

21. Gabutti, B., (1983), "On Two Upwind Finite Difference Schemes for Hyperbolic Equations in Non-Conservation Form," *Computers and Fluids*, V.11, No.3, pp.207-230.

22. Gottlieb, D. and Orszag, S.A., (1977), *Numerical Analysis of Spectral Methods, Theory and Applications*, SIAM-CBMS Philadelphia.

23. Johnson, B.H., (1974), "Unsteady Flow Computations on the Ohio-Cumberland-Tennessee-Mississippi River System," *Tech. Report H-74-8*, Hydraulics Lab., Waterways Experiment Station, U.S. Army Corps of Engs., Vicksburg, Mississippi.

24. Katopodes, N.D. and Strelkoff, T., (1978), "Computing Two-Dimensional Dam-Break Flood Waves," *Jour. of Hyd. Div.*, A.S.C.E., V.104, No.9, September, pp.1269-1288.

25. Katopodes, N.D., (1980), "Finite Element Model for Open-Channel Flow Near Critical Conditions," *Finite Elements in Water Resources III*, S.Y. Wang, et al.,eds., Univ. of Mississippi Press, pp.5.37-5.46.

26. Katopodes, N.D., (1984), "a Dissipative Galerkin Scheme for Open-Channel Flow," *Jour. of Hyd. Eng.*, V.110, No.4, April, pp.450-465.

27. Katopodes, N.D., (1984), "Two-Dimensional Surges and Schocks in Open-Channels," *Jour. of Hyd. Div.*, A.S.C.E., V.110, No.6, June, pp.794-812.

28. Keuning, D.H., (1976), "Application of Finite Element Method to Open-Channel Flow," *Jour. of Hyd. Div.*, A.S.C.E., V.102, No.HY4, April, pp.459-468.

29. King, I.P., (1976), "Finite Element Models for Unsteady Flow Routing through Irregular Channels," *Finite Elements in Water Resources*, C.A. Brebbia, et al.,eds., Pentech press, London, pp.4.165-4.184.

30. Lax, P.D., (1954), "Weak Solution of Nonlinear Hyperbolic Partial Differential Equations and their Numerical Computation," *Comm. on Pure and Applied Mathematics*, V.7, pp.159-163.

31. Lax, P.D. and Wendroff, B., (1960), "Systems of Conservation Laws," *Comm. on Pure and Applied Mathematics*, V.13, pp.217-237.

32. Liggett, J.A. and Woolhiser, D.A., (1967), "Difference Solutions of Shallow-Water Equation," *Jour. of Eng. Mech. Div.*, A.S.C.E., V.93, No.EM2, April, pp.39-71.

33. Liggett, J.A. and Cunge, J.A., (1975), 'Numerical Methods of Solution of the Unsteady Flow Equations' In Mahmood, K. and Yevjevich, V.; Unsteady Flow in Open Channels, V.I, Fort Collins, Colorado: Water Res. Publiation, Chapter 4, pp.89-182.

34. MacCormack, R.W., (1969), "The Effect of Viscosity in Hypervelocity Impact Cratering," A.I.A.A., Paper 69-354, Cincinnati, Ohio.

35. Mahmood, K. and Yevjevich, V., (1975), *Unsteady flow in open channels, V.I and II*, Water Res. Publications, PO Box 303, Fort Collins, Colorado 80522, USA.

36. Martin, C.S. and DeFazio, F.G., (1969), "Open-Channel Surge Simulation by Digital Computer," *Jour. of Hyd. Div.*, A.S.C.E., V.95, No.HY6, November, pp.2049-2070.

37. Meissner, U., (1978), "An Explicit-Implicit Water-Level Model for Tidal Computations of Rivers," *Computer Methods in Applied Mech. and Eng.*, V.13, pp.221-232.

38. Moin, P. and Kim, J., (1980), "On the Numerical Solution of Time Dependent Viscous Incomprssible Fluid Flows involving Solid Boundaries," *Journ. of Computational Physics* 35, pp.381-392.

39. Orszag, S.A., (1980). "Spectral Methods for Problems in Complex Geometries," *Jour. of Computational Physics* 37, pp.70-92.

40. Stoker, J.J., (1953), "Numerical Solution of Flood Prediction and River Regulation Problems," New York Univ., Inst. Math. Sci. Report IMM-200.

41. Streeter, V.L. and Wylie, E.B., (1967), *Hydraulic Transients*, McGraw-Hill Book Company, New York.

42. Strelkoff, T., (1970), "Numerical Solution of St.-Venant Equations," *Jour. of Hyd. Div.*, A.S.C.E., V.96, No.HY1, January, pp.223-252.

43. U.S. Army Corps of Engineering, (1987), TABS-2, Open-Channel Flow and Sedimentation, Generalized Computer Program System, Waterways Experiment Station, Vicksburg.

44. Wylie, E.B., (1970), "Unsteady Free-Surface Flow Computation," *Jour. of Hyd. Div.*, A.S.C.E., V.96, No.HY11, November, pp.2241-2251.

APPENDIX A

Details of equation (2.3.2.1); for convenience the bar has been dropped from the barred variables without changing the nature of the variables.

Equation (2.3.2.1a);

$$h_1^{p+1} \cdot v_1^{p+1} - \left[1+(q_p-1)(t/t_p)^{[1/(t_r-1)]}\ \varepsilon^{[1-(t/t_p)][1-(t_r-1)]}\right]$$

Equation (2.3.2.1b);

$$\frac{a_o}{dt}\left\{\left(h_{j+1}^{p+1} + h_j^{p+1}\right) - \left(h_{j+1}^{p} + h_j^{p}\right)\right\}$$

$$+ \frac{b_o}{(x_{j+1} - x_j)}\left\{\alpha\left(v_{j+1}^{p+1} + v_j^{p+1}\right) + (1-\alpha)\left(v_{j+1}^{p} + v_j^{p}\right)\right\}$$

$$* \left\{\alpha\left(h_{j+1}^{p+1} - h_j^{p+1}\right) + (1-\alpha)\left(h_{j+1}^{p} - h_j^{p}\right)\right\}$$

$$+ \frac{c_o}{(x_{j+1} - x_j)}\left\{\alpha\left(h_{j+1}^{p+1} + h_j^{p+1}\right) + (1-\alpha)\left(h_{j+1}^{p} + h_j^{p}\right)\right\}$$

$$* \left\{\alpha\left(v_{j+1}^{p+1} - v_j^{p+1}\right) + (1-\alpha)\left(v_{j+1}^{p} - v_j^{p}\right)\right\} = 0 \ ; \quad 1 \le j \le N-1$$

Equation (2.3.2.1c);

$$\frac{d_o}{dt}\left\{\left(v_{j+1}^{p+1} + v_j^{p+1}\right) - \left(v_{j+1}^{p} + v_j^{p}\right)\right\}$$

$$+ \frac{e_o}{(x_{j+1} - x_j)} \{\alpha \left(v_{j+1}^{p+1} + v_j^{p+1}\right) + (1-\alpha) \left(v_{j+1}^{p} + v_j^{p}\right)\}$$

$$* \{\alpha \left(v_{j+1}^{p+1} - v_j^{p+1}\right) + (1-\alpha) \left(v_{j+1}^{p} - v_j^{p}\right)\}$$

$$+ \frac{2 f_o}{(x_{j+1} - x_j)} \{\alpha \left(h_{j+1}^{p+1} - h_j^{p+1}\right) + (1-\alpha) \left(h_{j+1}^{p} - h_j^{p}\right)\}$$

$$+ g_o S_o \{\alpha \left(S_{f_{j+1}}^{p+1} + S_{f_j}^{p+1}\right) + (1-\alpha) \left(S_{f_{j+1}}^{p} + S_{f_j}^{p}\right)\}$$

$$- 2 g_o S_o = 0 ; \qquad 1 \leq j \leq N-1$$

and

Equation (2.3.2.1d);

$$(x_N - x_{N-1}) h_{N-2}^{p+1} - (x_N - x_{N-2}) h_{N-1}^{p+1} + (x_{N-1} - x_{N-2}) h_N^{p+1} = 0$$

APPENDIX B

Details of matrix equation (2.3.2.3);

for convenience the bar has been dropped from the barred variables without changing the nature of the variables.

Elements of the coefficient matrix;

$$a_1^u \equiv h_1^{p+1}$$

$$b_1^u \equiv v_1^{p+1}$$

$$a_j^c \equiv \frac{a_o}{dt} - \frac{\alpha\, b_o}{(x_{j+1} - x_j)} \{\alpha \left(v_{j+1}^{p+1} + v_j^{p+1}\right) + (1-\alpha) \left(v_{j+1}^{p} + v_j^{p}\right)\}$$

$$+ \frac{\alpha\, c_o}{(x_{j+1} - x_j)} \{\alpha \left(v_{j+1}^{p+1} - v_j^{p+1}\right) + (1-\alpha) \left(v_{j+1}^{p} - v_j^{p}\right)\} ;$$

$$1 \le j \le N-1$$

$$b_j^c \equiv \frac{\alpha\, b_o}{(x_{j+1} - x_j)} \{\alpha \left(h_{j+1}^{p+1} - h_j^{p+1}\right) + (1-\alpha) \left(h_{j+1}^{p} - h_j^{p}\right)\}$$

$$- \frac{\alpha\, c_o}{(x_{j+1} - x_j)} \{\alpha \left(h_{j+1}^{p+1} + h_j^{p+1}\right) + (1-\alpha) \left(h_{j+1}^{p} + h_j^{p}\right)\} ;$$

$$1 \le j \le N-1$$

$$c_{j+1}^c \equiv \frac{a_o}{dt} + \frac{\alpha\, b_o}{(x_{j+1} - x_j)} \{\alpha \left(v_{j+1}^{p+1} + v_j^{p+1}\right) + (1-\alpha) \left(v_{j+1}^{p} + v_j^{p}\right)\}$$

$$+ \frac{\alpha\, c_o}{(x_{j+1} - x_j)} \{\alpha \left(v_{j+1}^{p+1} - v_j^{p+1}\right) + (1-\alpha) \left(v_{j+1}^{p} - v_j^{p}\right)\}$$

$$1 \le j \le N-1$$

$$d_{j+1}^c \equiv \frac{\alpha\, b_o}{(x_{j+1} - x_j)} \{\alpha \left(h_{j+1}^{p+1} - h_j^{p+1}\right) + (1-\alpha) \left(h_{j+1}^{p} - h_j^{p}\right)\}$$

$$+ \quad \frac{\alpha\, c_o}{(x_{j+1} - x_j)} \{\alpha\, (h_{j+1}^{p+1} + h_j^{p+1}) + (1-\alpha)\, (h_{j+1}^{p} + h_j^{p})\}$$

$$1 \le j \le N-1$$

$$a_j^m \equiv - \frac{2\, \alpha\, f_o}{(x_{j+1} - x_j)} - \frac{4}{3}\, \alpha\, g_o\, p_o\, n^2\, \frac{(v_j^{p+1})^2}{(h_j^{p+1})^{7/3}}; \qquad 1 \le j \le N-1$$

$$b_j^m \equiv \frac{d_o}{dt} - \frac{2\, \alpha\, e_o}{(x_{j+1} - x_j)} \{\alpha\, v_j^{p+1} + (1-\alpha) + v_j^{p}\}$$

$$+ \quad 2\, \alpha\, g_o\, p_o\, n^2\, \frac{(v_j^{p+1})}{(h_j^{p+1})^{4/3}} \qquad 1 \le j \le N-1$$

$$c_{j+1}^m \equiv \frac{2\, \alpha\, f_o}{(x_{j+1} - x_j)} - \frac{4}{3}\, \alpha\, g_o\, p_o\, n^2\, \frac{(v_{j+1}^{p+1})^2}{(h_{j+1}^{p+1})^{7/3}}; \qquad 1 \le j \le N-1$$

$$d_{j+1}^m \equiv \frac{d_o}{dt} + \frac{2\, \alpha\, e_o}{(x_{j+1} - x_j)} \{\alpha\, v_{j+1}^{p+1} + (1-\alpha) + v_{j+1}^{p}\}$$

$$+ 2\, \alpha\, g_o\, p_o\, n^2\, \frac{(v_{j+1}^{p+1})}{(h_{j+1}^{p+1})^{4/3}} \qquad 1 \le j \le N-1$$

$$c_{N-2}^d \equiv x_N - x_{N-1}$$

$$a_{N-1}^d \equiv x_{N-2} - x_N$$

$$c_N^d \equiv x_{N-1} - x_{N-2}$$

Elements of residual matrix (right hand matrix);

$$r_1^u \equiv h_1^{p+1}.v_1^{p+1} - \left[1+(q_p-1)(t/t_p)^{[1/(t_r-1)]}\ e^{[1-(t/t_p)][1-(t_r-1)]}\right]$$

$$r_j^c \equiv \frac{a_o}{dt}\{(h_{j+1}^{p+1} + h_j^{p+1}) - (h_{j+1}^{p} + h_j^{p})\}$$

$$+ \frac{b_o}{(x_{j+1} - x_j)}\{\alpha\,(v_{j+1}^{p+1} + v_j^{p+1}) + (1-\alpha)\,(v_{j+1}^{p} + v_j^{p})\}$$

$$* \{\alpha\,(h_{j+1}^{p+1} - h_j^{p+1}) + (1-\alpha)\,(h_{j+1}^{p} - h_j^{p})\}$$

$$+ \frac{c_o}{(x_{j+1} - x_j)}\{\alpha\,(h_{j+1}^{p+1} + h_j^{p+1}) + (1-\alpha)\,(h_{j+1}^{p} + h_j^{p})\}$$

$$* \{\alpha\,(v_{j+1}^{p+1} - v_j^{p+1}) + (1-\alpha)\,(v_{j+1}^{p} - v_j^{p})\}\ ;$$

$$1 \le j \le N-1$$

$$r_j^m \equiv \frac{d_o}{dt}\{(v_{j+1}^{p+1} + v_j^{p+1}) - (v_{j+1}^{p} + v_j^{p})\}$$

$$+ \frac{e_o}{(x_{j+1} - x_j)}\{\alpha\,(v_{j+1}^{p+1} + v_j^{p+1}) + (1-\alpha)\,(v_{j+1}^{p} + v_j^{p})\}$$

$$* \{\alpha\,(v_{j+1}^{p+1} - v_j^{p+1}) + (1-\alpha)\,(v_{j+1}^{p} - v_j^{p})\}$$

$$+ \frac{2\,f_o}{(x_{j+1} - x_j)}\{\alpha\,(h_{j+1}^{p+1} - h_j^{p+1}) + (1-\alpha)\,(h_{j+1}^{p} - h_j^{p})\}$$

$$+ g_o\,S_o\,\{\alpha\,(S_{f_{j+1}}^{p+1} + S_{f_j}^{p+1}) + (1-\alpha)\,(S_{f_{j+1}}^{p} + S_{f_j}^{p})\}$$

$$- 2\,g_o\,S_o\ ; \qquad 1 \le j \le N-1$$

$$r_N^d \equiv (x_N - x_{N-1})\,h_{N-2}^{p+1} - (x_N - x_{N-2})\,h_{N-1}^{p+1} + (x_{N-1} - x_{N-2})\,h_N^{p+1}$$